TI Designs: TIDA-03050
Automotive, mA-to-kA Range, Current Shunt Sensor Reference Design

Description

This reference design shows how to detect current from the mA-to-KA range using a busbar-type shunt resistor. The increasing demand of high-capacity batteries in electric vehicles (EVs) and hybrid electric vehicles (HEVs) drives the requirement for larger current spans and highly-accurate current sensors. Obtaining a good accuracy over three decades (mA to A, 1 A to 100 A, and 100 A to 1000 A) is quite challenging due to large amounts of noise in the system. This design solves this problem by using a high-resolution analog-to-digital converter (ADC) and high-accuracy current shunt monitors from TI.

Resources

TIDA-03050	Design Folder
ADS1259-Q1	Product Folder
INA240-Q1	Product Folder
OPA320-Q1	Product Folder
LMT01-Q1	Product Folder
TPS709-Q1	Product Folder
TIDA-03040	Product Folder

TI E2E™ Community — ASK Our E2E Experts

Features

- Full-Scale Accuracy of:
  - 0.02% Full-Scale Range (FSR) for < 20 A and < 0.05% FSR for 20 A to 1500 A at 25°C
  - 0.1% FSR for < 20 A and 0.25% FSR for 20 A to 1500 A at 50°C
- Suitable for 200-mA to 1200-A Range Current Measurement; Configurable to Varied Current Spans
- High-Side Sensing and Low-Side Sensing
- Supports Bidirectional Current
- Bidirectional Current Measurement: –1500 A to +1500 A

Applications

- Current Sensing in 12-V, 48-V, and 400-V Battery Management Systems (BMS)

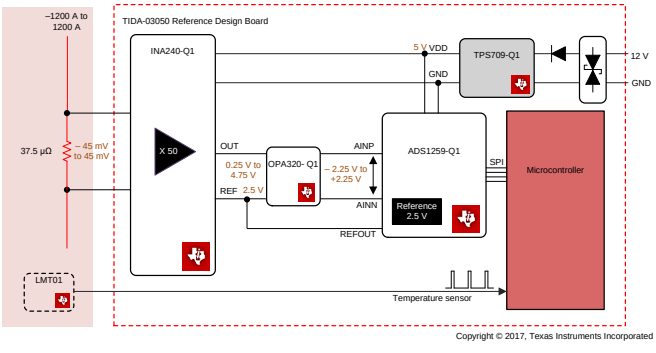

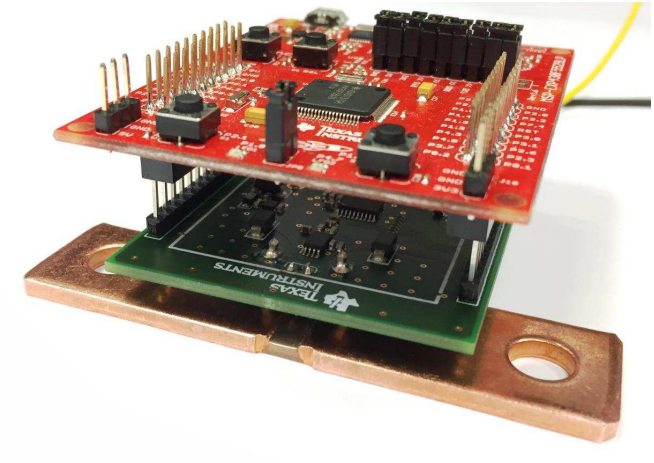

An IMPORTANT NOTICE at the end of this TI reference design addresses authorized use, intellectual property matters and other important disclaimers and information.

1 System Description

At the time of this writing, hybrid and electrical vehicles are paving the way for electrification in the automotive sector. The main source of energy for these vehicles is the battery, monitoring, and control of the battery management system (BMS), which plays a critical role in vehicle electrification. Monitoring the critical parameters, such as the state-of-health (SOH) and state-of-charge (SOC) of the battery, requires different types of sensor information such as voltage sensors, temperature sensors, current sensors, and so forth. This reference design focuses on the signal conditioning of battery current sensors. The performance of any current sensor solution mainly depends on the device specifications such as accuracy, bandwidth, linearity, and precision. Designing a system that satisfies all the required specifications is a challenging task. This reference design provides a way to handle these parameters using TI's current shunt monitors and ADCs.

Designers have several methods for measuring current, such as Faraday's induction law, Ohm's law, Lorentz force law, magneto-resistance effect, magnetic saturation, and many other principles. This reference design is based on Ohm's law (shunt current sensing). Shunt technology continues to be widely adapted for measuring currents in HEVs and EVs due to the advancements in low-value precision shunts and huge improvements to analog front-end (AFE) circuits. For example, shunts from Vishay and Isabellenhütte Heusler GmbH & Co. KG offer very-low resistance values (35 μΩ, 50 μΩ, 100 μΩ, 125 μΩ, and 500 μΩ). With these lower values of shunts, the voltage drop across the shunt is very small. The signal conditioning must offer very-low noise and a highly-accurate front end to measure such a tiny voltage drop.

A clear understanding on which kind of topology to use is essential when designing the current sensor front end. Table 1 shows the features offered by the TIDA-03050 design.

Table 1. TIDA-03050 Benefits

GENERAL PARAMETERS	TIDA-03050 BENEFITS
Low side and high side	Suitable for both low-side and high-side systems depending on the battery voltage
Unidirectional or bidirectional	Bidirectional; can also be configured for unidirectional applications
Current sensing range	–1200 A to 1200 A
Accuracy	< 0.02% FSR for < 20 A and < 0.05% FSR for 20 A to 1500 A at 25°C
Bandwidth	3.6 kSPS, 14.4 kSPS

Parameters of the battery current sensor vary depending on the vehicle requirements set by the manufacturers.

This reference design targets higher accuracies for larger current span ranges. A high current of ±1200 A is made to pass through a shunt of 37.5 μΩ, which results in a voltage drop of –45 mV to +45 mV across the shunt resistor. This four-wire shunt resistor is connected in a Kelvin connection to the TI's current shunt monitor (INA240-Q1). The INA240 shunt monitor captures the differential signal and amplifies it with a gain of 50 V/V (and with a reference of 2.5 V), which results in an output of 0.25 V to 4.75 V. The buffer stage is preceded by the INA240 and OPA320-Q1 devices and is used in a buffer configuration, which helps to match the output impedance of the INA240 device with the RC filter and the high-resolution ADC (ADS1259-Q1). The ADC accepts the output from the charged RC filter cap and initially modulates the signal at 950 MHz. The delta sigma (ΔΣ) modulator has an inside decimator which is specified at different output data rates: 10 samples per second (SPS) to 14.4 kSPS. The $sinc^1$ and $sinc^2$ filters precede the decimator and the MSP430F5529 MCU extracts the final output through a USB for further signal processing.

The performance of any current sensor solution mainly depends on the device specifications such as accuracy, bandwidth, linearity, precision, and efficiency. Designing a system that satisfies all the required specifications is a challenging task. This reference design shows how to address these parameters to obtain the most accuracy from a current sensor.

1.1 Key System Specifications

Table 2. Key System Specifications

PARAMETER	SPECIFICATIONS
Measurement parameter	Current
Sensor type	Shunt (resistive)
Shunt value	37.5 µΩ
Power supply	12 V
Current consumption	6 mA (except MCU)
ADC	24-bit delta sigma (ΔΣ)
Overvoltage protection	Yes
Reverse polarity protection	Yes
operating temperature	–40°C to +125°C
Calibration	Offset and gain calibration
Output	Digital
Form factor	45x55-mm rectangular PCB

2 System Overview

2.1 Block Diagram

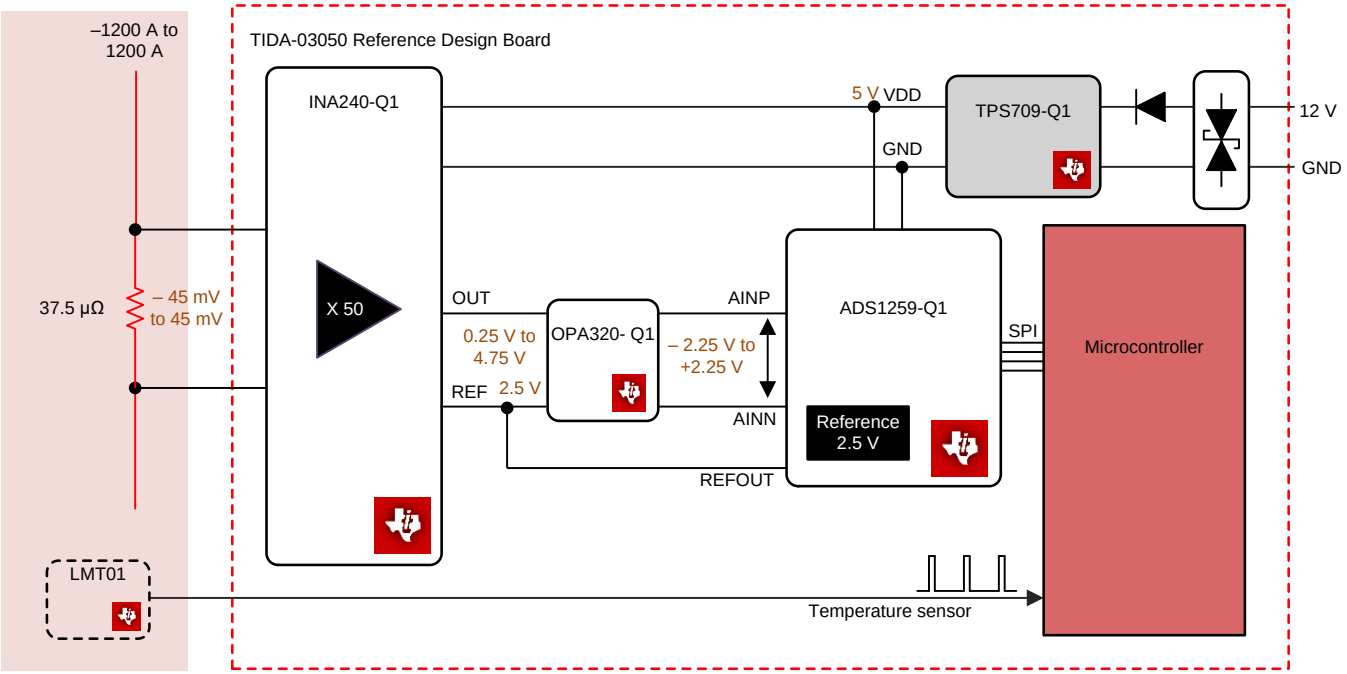

Figure 1. TIDA-03050 Block Diagram

Figure 2 shows the total system represented in four connected blocks (orange, green, light green, and gray):

- Current shunt monitor (INA240): Current shunt monitor functions to amplify the voltage across the shunt (orange block)
- Buffer stage (OPA320-Q1): Buffer amplifier for use to match the output impedances of INA240 with ADS1259-Q1 (green block)
- Power stage (TPS709-Q1): Low-dropout regulator (LDO) supplies regulated voltage to the INA240 and ADS1259-Q1 (light green block)
- Conversion stage (ADS1259-Q1): ADC digitizes the signals with low noise, high resolution, high speed, and high accuracy (gray block)

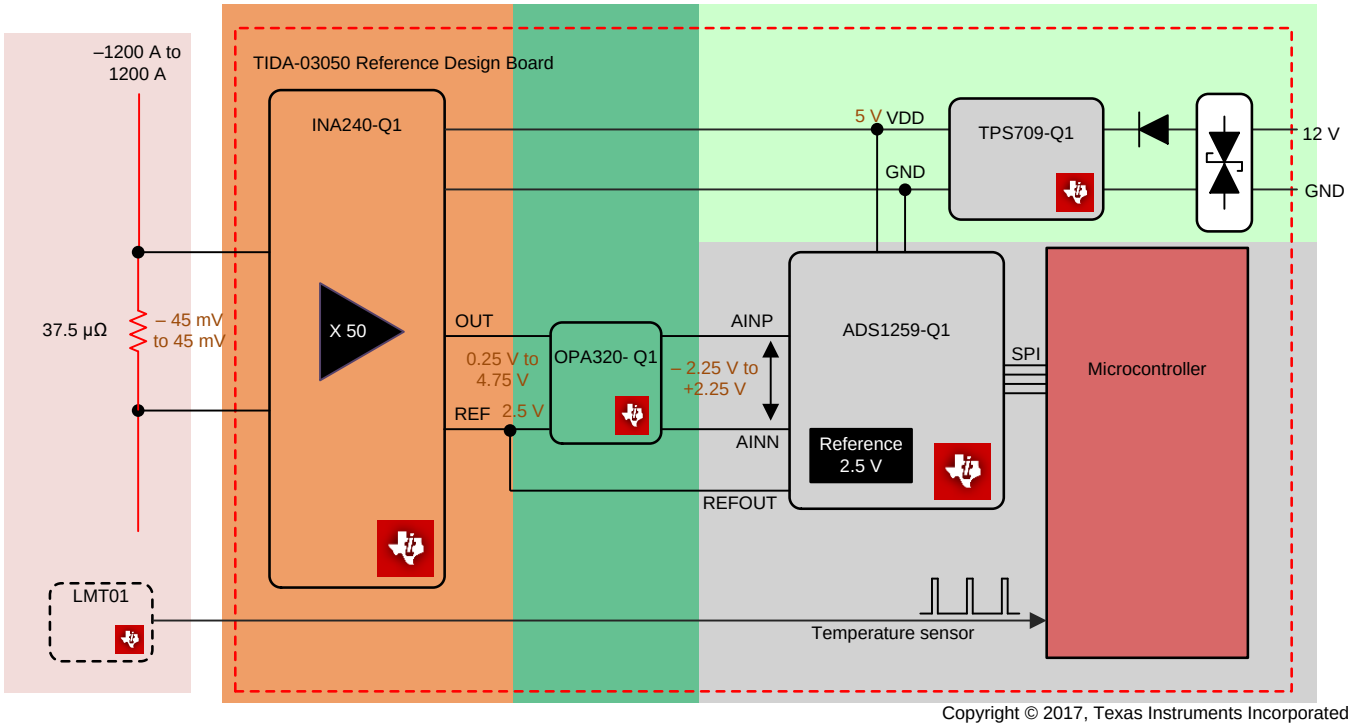

Figure 2. Functional Block Diagram

2.2 Highlighted Products

2.2.1 ADS1259-Q1

The noise in a system limits the current sensor system from obtaining higher accuracy. Thermal and quantization noise are not calibratable sources of ADC noise. The use of a high-resolution ADC, however, allows the designer to reduce quantization noise. A high-resolution ADC is especially necessary in this reference design because of the wider spans of current ranges (1 mA to 1 A, 1 A to 100 A, and 100 A to 1000 A). Using a high-resolution ADC, such as the ADS1259-Q1, is preferable to effectively provide accuracy over all three decades.

The ADS1259-Q1 is a high-linearity, low drift, 24-bit ADC designed to meet the requirements of high-precision, high-accuracy applications. The device can perform conversions at data rates up to 14.4 kSPS with high resolution and is therefore ideally suited to measure rapidly-changing signals that have a wide dynamic range. An integrated low-noise, low-drift 2.5-V voltage reference is also used as a reference of the INA240 device. The reference changes ratiometrically to the output of INA240 to completely eliminate drift error. The converter uses a fourth-order, inherently stable $\Delta\sum$ modulator that provides excellent noise

performance and linearity. A fast-responding input overrange detector flags the conversion data if an input overrange event occurs. To augment data integrity in noisy automotive environments, the ADS1259-Q1 offers an optional checksum byte and a redundant conversion data-read capability. The ADS1259-Q1 consumes 13 mW during operation and less than 25 μW when powered down. TI offers the ADS1259-Q1 device in a TSSOP-20 package with a full specification from –40°C to 125°C.

The key features of this device are as follows:

- Qualified for automotive applications AEC-Q100
- Temperature grade 1: –40°C to 125°C
- Programmable data rates: 10 SPS to 14.4 kSPS
- Internal reference: 2.5 V, 10-ppm/°C drift
- Analog supply: 5 V or ±2.5 V
- Digital supply: 2.7 V to 5 V
- High performance:
  - 21.3 effective number of bits (ENOB) at 1.2 kSPS
  - Integral nonlinearity (INL): 3 ppm
  - Offset drift: 0.05 μV/°C
  - Gain drift: 0.5 ppm/°C

2.2.2 INA240-Q1

Selecting the right current monitor is essential because of the noise specifications at lower currents. INA240 offers very low offset and gain drifts with chopper-stabilized front-end operation. The INA240 is a voltage-output, current-sense amplifier. The device is able to sense drops across shunt resistors over a wide common-mode voltage range from –4 V to 80 V, independent of the supply voltage. The negative common-mode voltage allows the device to operate below ground, which implies that this monitor is suitable for low-side sensing, as well. This device operates from a single 2.7-V to 5.5-V power supply, drawing a maximum of 2.4 mA of supply current. The device is able to sense even smaller voltages due to its 5-μV offset error (typical).

An excellent common-mode rejection ratio (CMRR), compatibility with low sides and high sides, and bidirectional features make this a good device for this application. The device is also available in a TSSOP package.

The key features of this device are as follows:

- Excellent CMRR:
  - 132-dB DC CMRR
  - 93-dB AC CMRR at 50 kHz
- Wide common-mode range: –4 V to 80 V
- Accuracy:
  - Gain error: 0.20% (maximum)
  - Gain drift: 2.5 ppm/°C (maximum)
  - Offset voltage: ±25 μV (maximum)
  - Offset drift: 250 nV/°C (maximum)
- Quiescent current (I_Q): 2.4 mA (max)
- Bidirectional sensing using reference pin configuration
- Available gains: 20, 50, 100, and 200
- AECQ100 qualified
- Device temperature grade 1: –40°C to 125°C ambient operating temperature

2.2.3 OPA320-Q1

The OPA320-Q1 is used as a buffer amplifier in this reference design. A wide bandwidth, low noise, high input impedance, and low output impedance make the OPA320-Q1 perfectly suitable for use as a buffer amplifier to match the INA240 and ADS1259-Q1 stages.

The key features of this device are as follows:

- AEC Q100 qualified with grade 1 temperature rage (–40°C to +125°C)
- Precision with zero-crossover distortion
- Low input bias current: 0.9 pA (maximum)
- Low noise: 7 nV/vHz at 10 kHz
- Wide bandwidth: 20 MHz
- Slew rate: 10 V/µs
- Unity-gain stable
- Small VSSOP package

2.2.4 TPS709-Q1

The TPS709-Q1 series of linear regulators are ultra-low quiescent current devices designed for power-sensitive applications. A precision band gap and error amplifier provides 2% accuracy over temperature. A quiescent current of only 1 µA makes these devices ideal solutions for battery-powered, always-on systems that require very little idle-state power dissipation. These devices have thermal-shutdown, current-limit, and reverse-current protections for added safety.

These regulators can be put into shutdown mode by pulling the EN pin low. The shutdown current in this mode goes down to 150 nA, typical. The TPS709-Q1 series is available in WSON-6 and SOT-23-5 packages.

The key features of this device are as follows:

- Qualified for automotive applications
- Grade 1
- Input voltage range: 2.7 V to 30 V
- Ultra-low quiescent current (I_Q): 1 µA
- Reverse current protection
- Low $I_{SHUTDOWN}$: 150 nA
- Supports 200-mA peak output
- 2% accuracy over temperature
- Available in fixed-output voltages: 1.2 V to 6.5 V
- Thermal shutdown and overcurrent protection

2.3 System Design Theory

EVs and HEVs are increasing in popularity. These vehicles provide several performance and ecological advantages over conventional vehicles. Most EV and HEV vehicles implement a stack of batteries containing many cells. The voltage level of the battery stacks vary depending on the vehicle requirements set by the manufacturers. The primary objective of the BMS is to provide an optimum solution for monitoring important parameters of automotive battery packs; one such important parameter is the current measurement. A real-time monitoring system for the battery stack is necessary to prevent the dynamics of battery such as shorts, overvoltage, overcurrent, overload damage, and so forth. The battery current, voltage, and other parameters must be measured with good accuracies over temperature ranges. This reference design aims to provide higher accuracies. A precision current-shunt resistor is used to transform input battery current into an analog voltage signal. A precision signal-conditioning circuit amplifies and adjusts the sensed voltage across the shunt and then feeds it into the input of the $\Delta\sum$ ADC for further signal processing.

The BMS is mainly used to estimate SOH and SOC. Integrating accurate sensors into the BMS is important to obtain detailed information about the SOH and SOC. For a typical battery, the current-, voltage-, and temperature sensors measure the following parameters in addition to protecting the battery from damage:

- Current flowing into the battery when charging or out of the battery when discharging
- Pack voltage
- Individual cell voltages
- Temperature of the cells

Use current sensors, voltage sensors, and temperature sensors to measure the these parameters and protect the battery from damage. See *Automotive Shunt-Based ±500-A Precision Current Sensing Reference Design* (TIDUCJ6) for more information about current sensors and their characterization. Figure 3 shows the location of current sensors in a block diagram of a battery control unit.

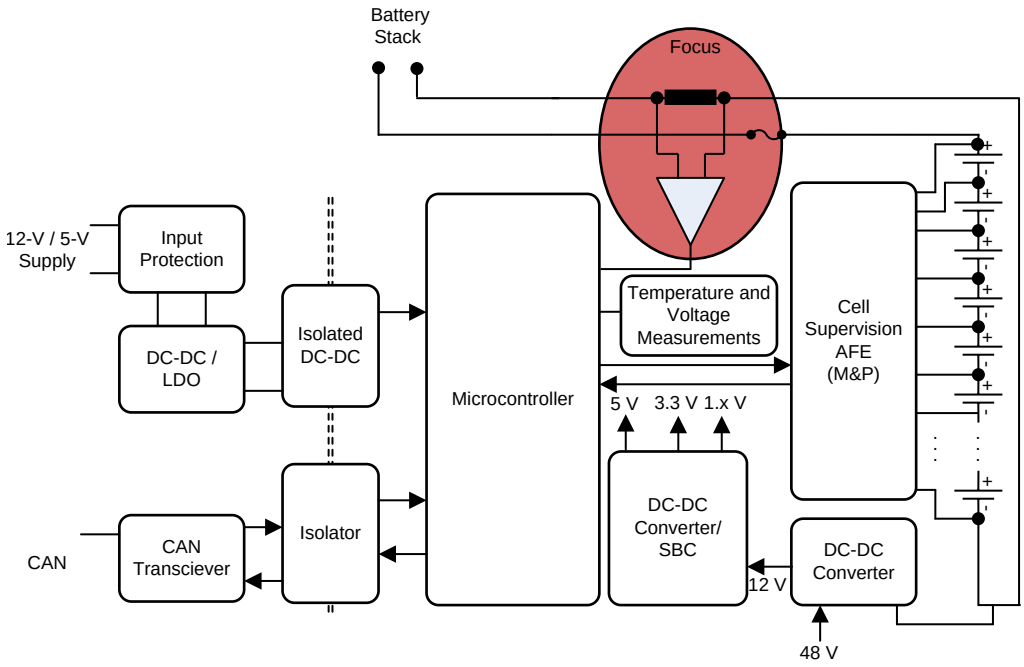

Figure 3. Current Sensor Location in Battery Control Unit

Information on charging and discharging cycles is essential to have when using a battery as the main source of energy in an HEV or EV system. Current sensors are the main source of information for charging and discharging cycles and work by reporting the status of the battery SOH to the BMS. Current sensors are usually located onboard or externally. With the increase of battery capacities in HEVs and EVs, the requirements for higher current ranges are increasing. The main requirements for a typical current sensor in HEVs and EVs are as follows:

- Current range from mA to kA:

  An example current range is 2000 A to 2000 A, –1200 A to 1200 A, and –500 A to 500 A. Higher current ranges are required to accommodate larger battery capacities, monitor dynamics of the load such as peak current detection (shorts-to-battery or shorts-to-ground), and satisfy initial start-up or torque demands.

- Higher bandwidths:

  Higher bandwidths are required to monitor the dynamics of the load or respond to fault states. Peak currents are in the kA range and last from milliseconds to a few seconds.

- High accuracy:

  The ability for a BMS to accurately measure parameters such as pack voltage, charging and discharging current, individual cell voltages, battery disconnection in abnormal conditions, charge stored by each cell in a stack, operational status of system components for assistance with functional safety, SOC, SOH, and state-of-function (SOF) all depend on the accuracy of the sensor inputs. The accuracy of the current sensor is important, especially at lower currents, so as to make very prompt decisions and increase system efficiency. Accuracy is usually specified separately for lower and higher currents.

- Temperature and linearity compensation:

  Temperature and linearity are critical factors in current sensors because of their dependency on temperature. Temperature dependency on the system results in poor accuracy. Maintaining the same accuracy over the entire temperature range is essential. Satisfying this requirement requires a temperature and compensation algorithm, which the user can implement on the onboard controller.

With these requirements in mind, this reference design is targeted for use in high-accuracy and high-precision applications. In shunt current sensors, a limited amount of current passes through a bus-bar-type shunt resistor and an AFE amplifier measures the voltage drop. Shunt technology continues to be widely adapted for measuring currents in HEVs and EVs due to advancements in low-value precision shunts and huge improvements in AFE circuits. For example, shunts from Vishay offer-very low resistance values (50 μΩ, 100 μΩ, 125 μΩ, and 500 μΩ). Using these lower-value shunts limits the voltage drop across the shunt to a very small amount. The challenge then is to measure this tiny voltage drop. TI's automotive current sensors provide complete solutions for these type of precision systems. Figure 4 shows the total system, which is divided into five sections (tan, orange, green, light green, and gray).

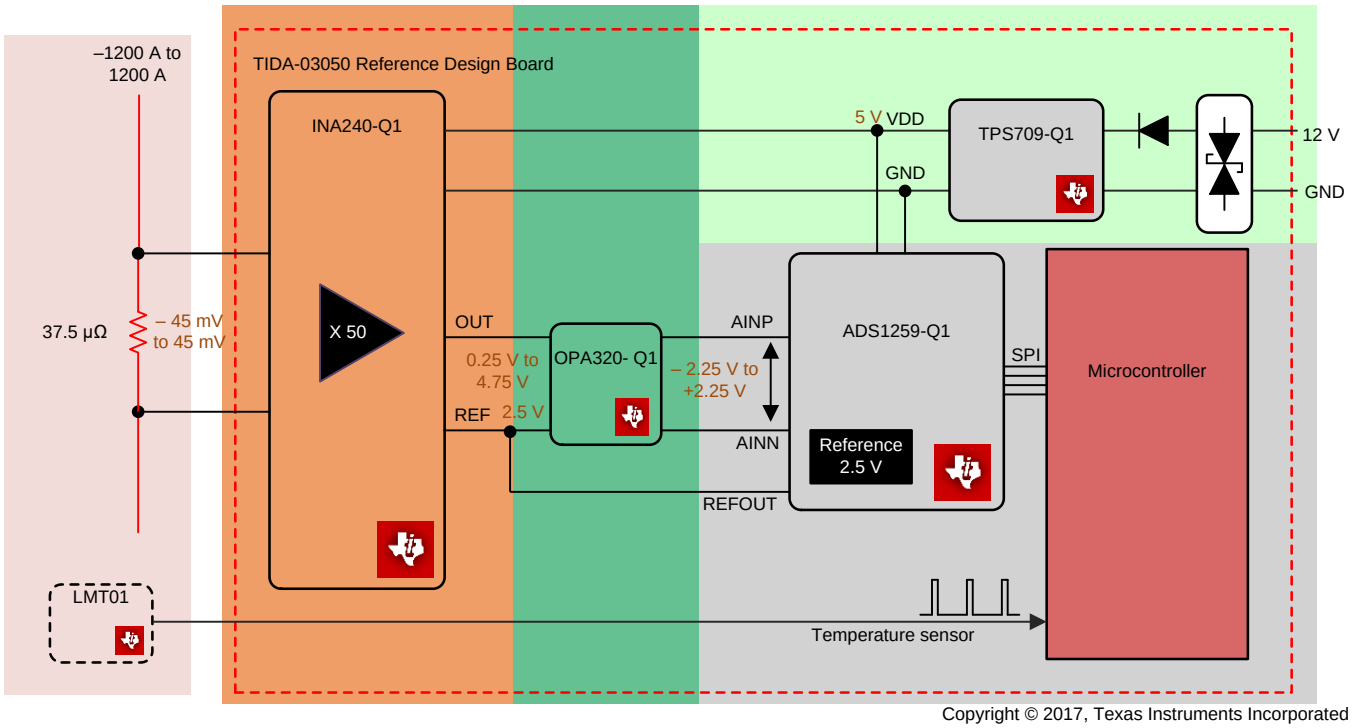

Figure 4. Sections Block Diagram

See *Automotive Shunt-Based ±500-A Precision Current Sensing Reference Design* (TIDUCJ6) for a similar current sensor solution.

2.3.1 Shunt Resistor Stage

The selection criteria and trade-offs for selecting a current shunt resistor are as follows:

- Increasing the shunt resistance value increases the voltage drop on the shunt, which helps to lower the requirements on the voltage offset (VOS) and input bias current offset (OSI) of the back-end amplifier. The trade-off, however, is that a larger value of shunt resistance can produce self-heating resulting from increased power dissipation. The temperature drift changes the nominal resistance of the shunt, which then affects the measurement accuracy.
- Using a smaller value of shunt resistance requires a larger gain configuration on the amplifier to match the full dynamic range of the ADC, which results in higher noise and affects overall system accuracy. Another critical requirement is to select a shunt resistor with a low temperature coefficient and tolerance because these parameters have a direct impact on the measurement accuracy.
- R = 37.5 µΩ
- I = 1500 A (maximum peak)

Based on the selection criteria and trade-offs, this reference design requires the selection of a very-low value shunt when considering that HEV and EV battery capacities are typically larger and thus have larger current ranges. This design uses a shunt from Isabellenhütte Heusler GmbH & Co. KG to satisfy these requirements, which features a 30-W power capability and a shunt value of 37.5 µΩ.

The smaller the pulse width is, the lower the power dissipation is in current sensors. Due to cranking conditions, a pulse with high current lasts for several milliseconds (typically < 50 ms); therefore, as Figure 5 shows, the pulse energy and pulse power are in the required limits.

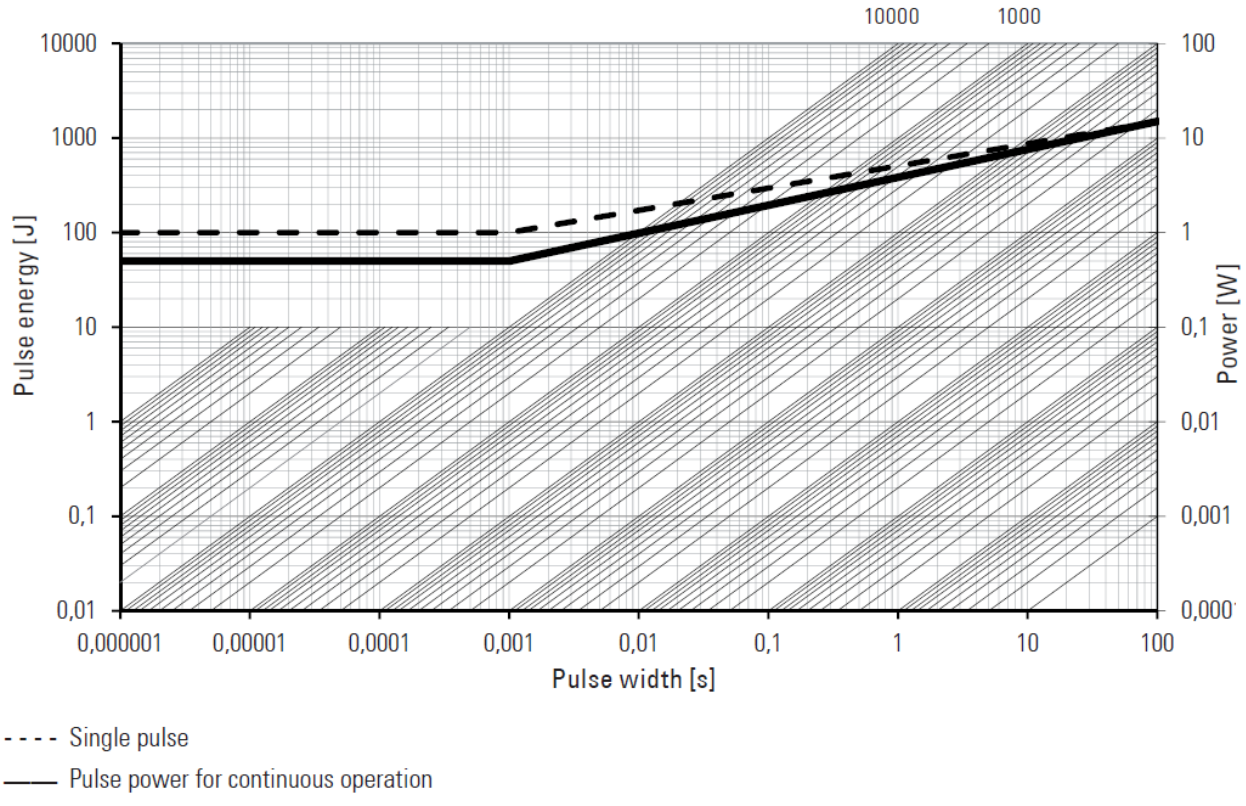

Figure 5. Maximum Pulse Energy and Power for Varied Pulse Widths

NOTE: This curve is only valid for the resistance value R0001. The shape of the curve in the range below 0.1 s will vary for other resistance values. This curve shows the approximate value; be sure to make a unique qualification for any pulse power measurement close to the above curve.

Figure 6 shows a four-terminal shunt. Two end terminals connect to the larger battery cables and the inner portion of the shunt connects to the INA240 device using a Kelvin connection. Figure 7 shows the four-terminal shunt conceptual diagram, where current flows through two terminals of the shunt and another two terminals are connected to the amplifier section.

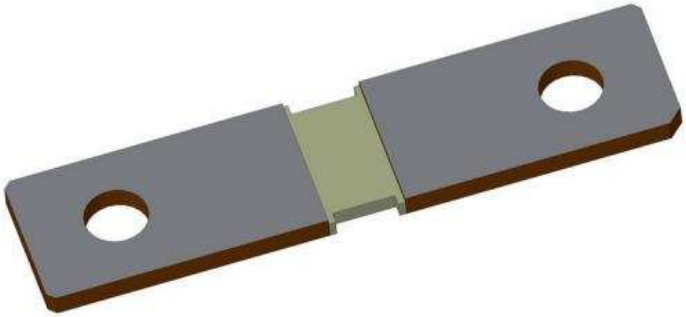

Figure 6. Shunt Real Image

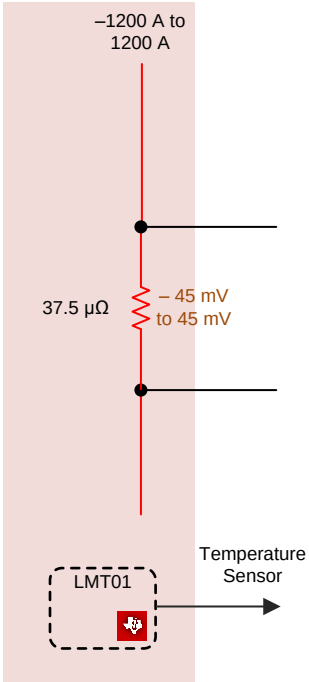

Figure 7. Shunt Resistor Circuit

The accuracy of a current sensor system depends mainly on the tolerance and temperature dependency of the shunt. A larger error contribution to the shunt is a result of shunt tolerances. Eliminate shunt tolerances by using compensation techniques. To perform compensation, use a LMT01 temperature sensor to detect the temperature of the shunt. Extract this temperature information to the MCU and then perform a compensation algorithm. Figure 8 shows the resistance versus temperature change plot of the Isabellahaute shunt at different temperature coefficient resistance (TCR) values.

As Equation 1 shows, when 1300 A of current flows through the 37.5-Ω resistor, the resulting differential voltage is 48.75 mV.

$$V = I \times R$$
$$V = \pm 1300 \times 37.5\ \mu\Omega$$
$$V = \pm 48.75\ mV \quad (1)$$

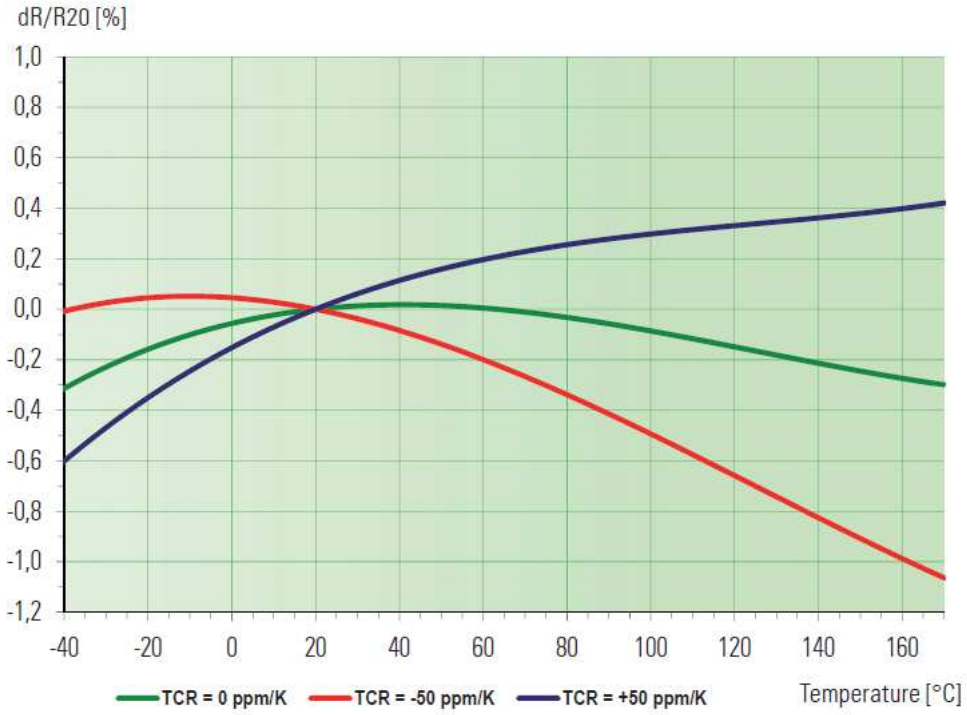

Figure 8. Resistance Change With Respect to Temperation Variations

2.3.2 Amplification Stage

As described in Section 2.3.1, shunt values must be low enough to pass through higher currents with a lower power dissipation. With these lower values of shunts, the voltage drop across the shunt is very small. When measuring this tiny voltage drop, in an ideal scenario the signal-conditioning front end has zero offset, zero input bias currents, zero gain error, and zero noise, which are the main parameters to consider when selecting an amplifier for battery current sensing. The amplifier specifications are critical because when lower currents flow through the lower shunt value, the resulting voltage drop is comparatively lower (in terms of µV). Differentiating the signal and noise is difficult when the offset and noise are also in the range of µV. In consideration of these requirements, this design selects the INA240 because it offers optimal performance in this application and provides accurate results. Figure 9 shows the current shunt monitor (INA240) connection to the shunt resistor.

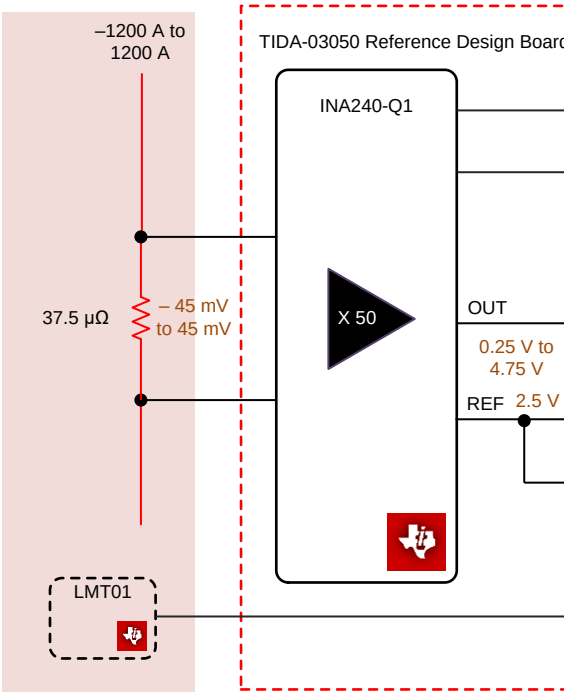

Figure 9. Current Shunt Monitor Section

As Figure 9 shows, when 1200 A flows through the 37.5-µΩ shunt, the voltage drop across the shunt registers from –45 mV to +45 mV (for a –1200-A to +1200-A current range).

The INA240 amplifier senses the voltage in between –45 mV to +45 mV in a differential configuration. The common-mode voltage of the INA240 is 80 V (max), which implies that a shunt can be connected to the high side for 12-V or 48-V systems and the remaining high-voltage configurations can be used with low-side configurations. INA240 has a gain factor 50 V/V, with which it provides an output between 0.25 V to 4.75 V. The INA240 device accepts both positive and negative currents because it has a reference voltage of 2.5 V, which means the absolute zero output of the INA240 is 2.5 V, the negative current falls below 2.5 V, and the positive currents rise above 2.5 V. The ADS1259-Q1 internal reference output generates this 2.5 V.

Figure 10 shows the INA240 schematic. Two transient voltage suppression (TVS) diodes connect to the two ends of the shunt to protect the signal line from transients (TVS specifications vary depending on the chosen environment). Assuming a 48-V system, select the breakdown voltage of the TVS as 58.1 V to prevent it from clamping before this value. Each TVS diode is capable of handling 600 W, which means that they can withstand 1200 W of power. Adjust the TVS diode power rating depending on the required protection level.

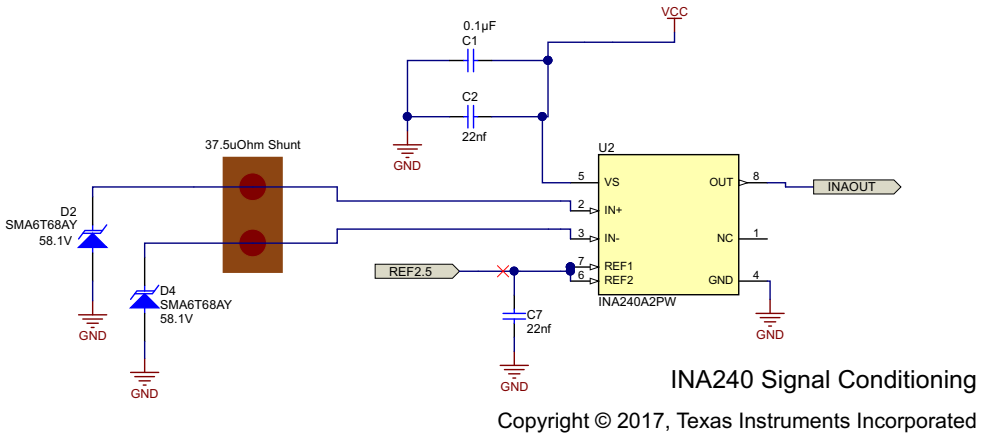

Figure 10. INA240 Schematics

Because a current shunt monitor is the first stage of amplification and offers 50 V/V, the current measurement accuracy is highly limited by the shunt amplifier. For this reason, an appropriate precision amplifier is necessary for a current shunt measurement with higher accuracy. The key specifications for the amplifier selection are as follows:

- Low input offset:

  Input offset voltage is typically the biggest factor that affects the system accuracy when measuring current. This offset occurs because the shunt output voltage is typically very small, generally in the order of µV, due to which the amplifier offset has a big impact on the measurement accuracy.
- Low offset drift:

  Offset drift is critical to maintain the system accuracy over temperature. Minimizing the drift is also important because calibrating drift error is very complicated and may require additional hardware.
- Low bias current:

  The input bias current of the amplifier affects the current that flows through the shunt, and thus affects the voltage drop across the shunt. For this reason, use amplifiers with low input bias current for better system accuracy.
- Low noise:

  The inherent noise of an amplifier can also affect the measurement accuracy, especially when configuring the amplifier with a higher noise gain.
- Small-signal bandwidth:

  This bandwidth should guarantee no attenuation of the input signal.

2.3.2.1 Buffer Amplifier Stage

A buffer amplifier is inserted between the INA240 and ADS1259-Q1 devices. A buffer amplifier helps to match the impedance between the INA240 and ADS1259-Q1. The following simulations made using TINA-TI™ software show the effect on the signal output of the INA240 with and without the use of a buffer amplifier. Figure 11 shows the OPA320-Q1 buffer amplifier. The input of the buffer amplifier is 0.25 V to 4.75 V and results in the same output to the ADC. The buffer amplifier output produces –2.25 V to +2.25 V for the ADC.

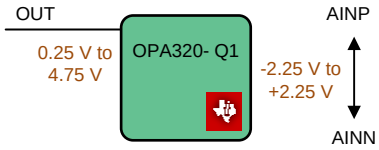

Figure 11. OPA320-Q1 Buffer Amplifier Block

The TINA-TI simulation in Figure 12 shows the output impedance block of the INA240-Q1 device. This simulation has been performed using the actual INA240 output impedance, as Figure 13 shows. This simulation shows the output impedance block (Zout) through VF1 connected to the ADS1259-Q1 with and without a buffer amplifier.

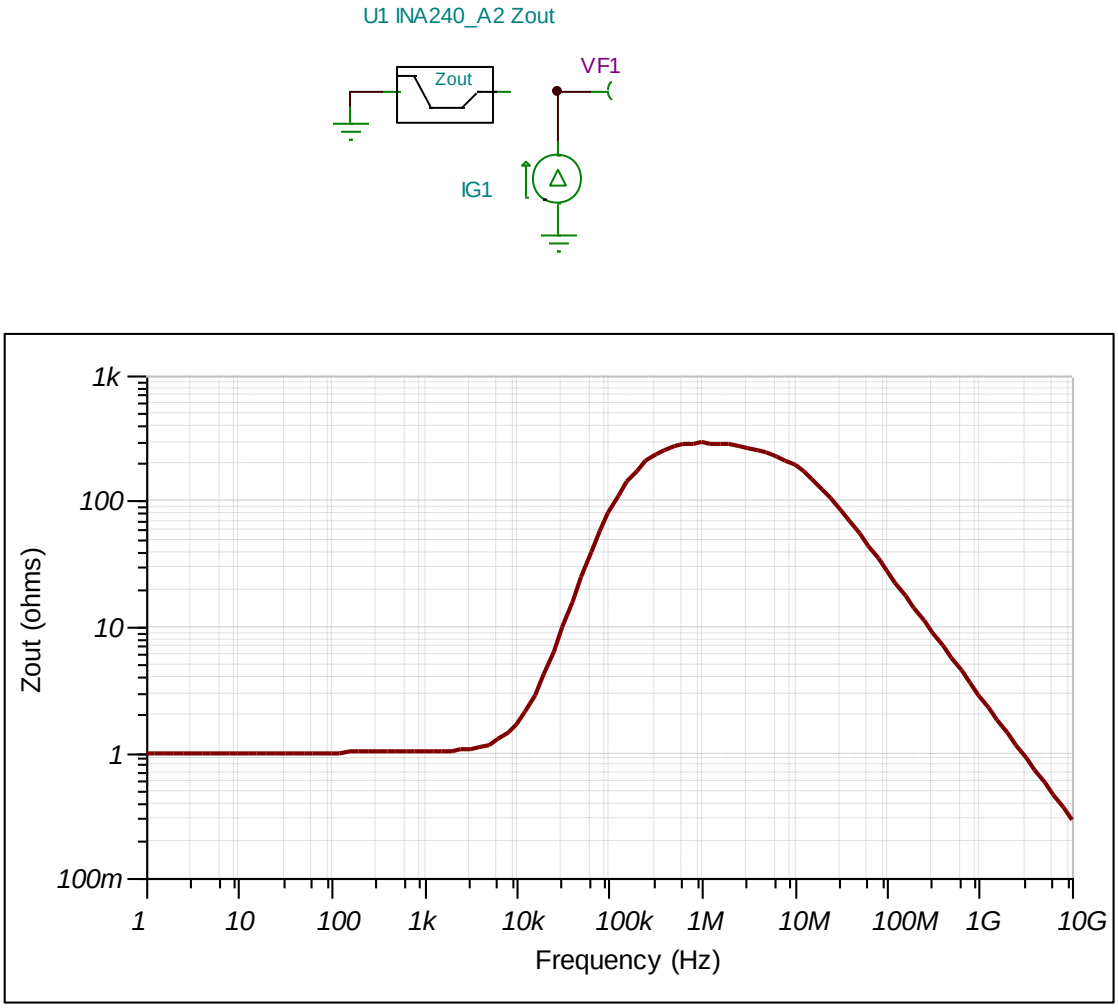

Figure 12. INA240 Output Impedance Block Realization in INA240

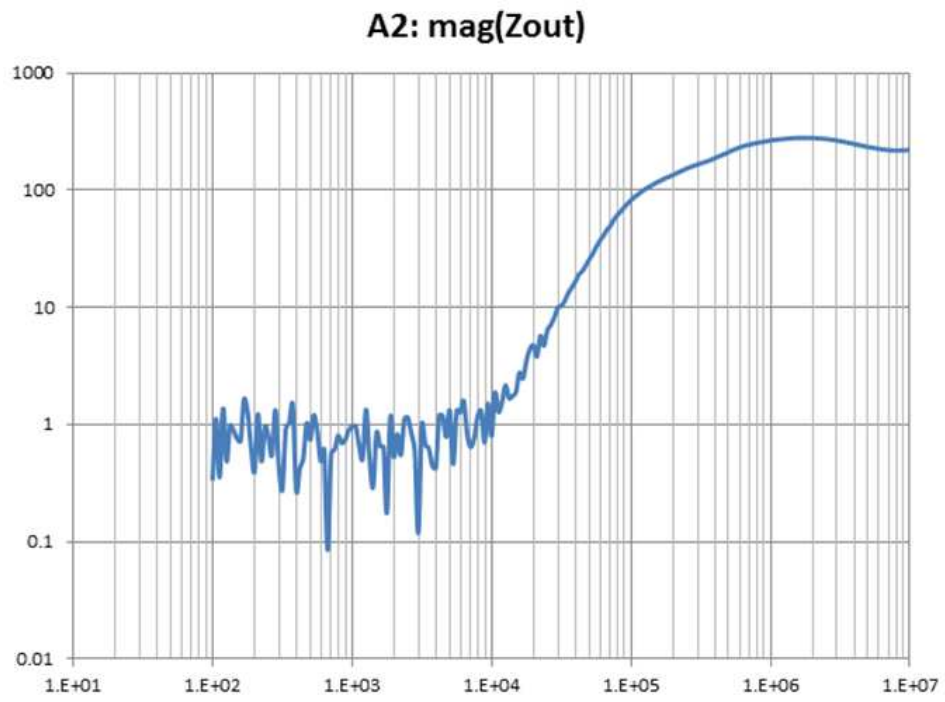

Figure 13. Output Impedance From INA240 Device (Real)

Figure 14 and Figure 15 show a simulation of connecting the INA240 output to ADS1259. Figure 14 shows a simulation of the INA240 output directly connected to the ADS1259-Q1 and Figure 15 shows the simulation of the INA240 output connected through a buffer amplifier.

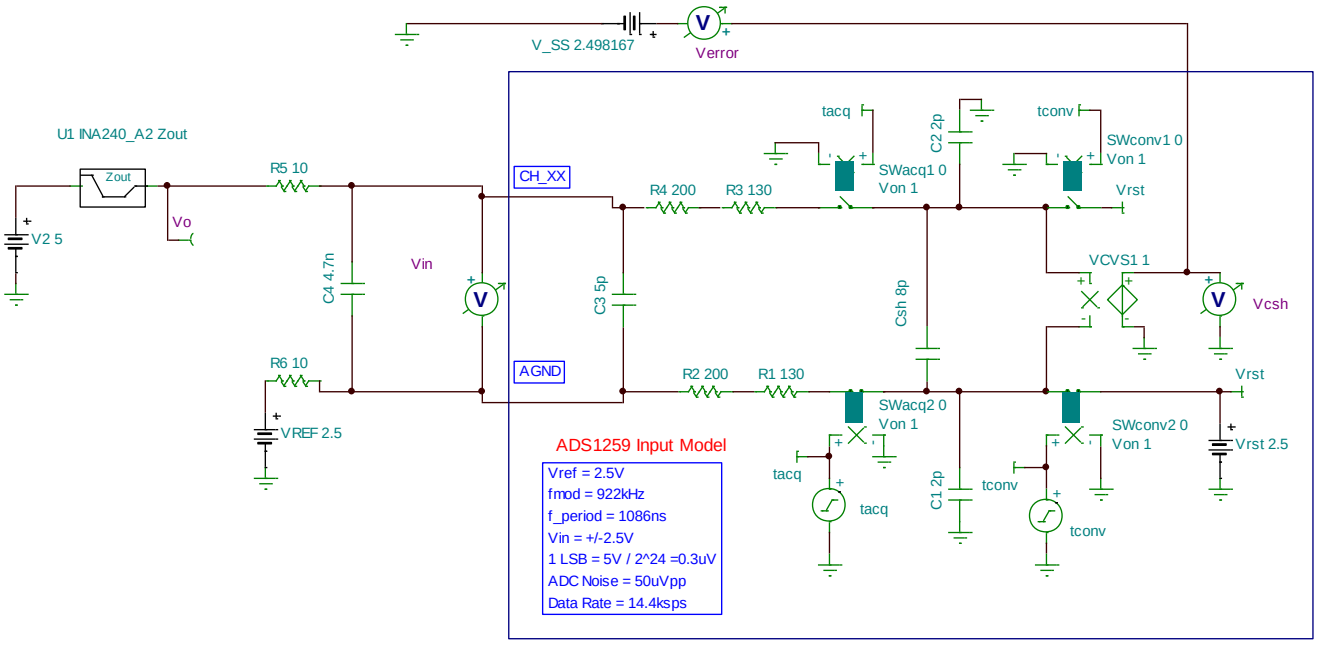

Figure 14. INA240 Output Directly Connected to ADS1259-Q1

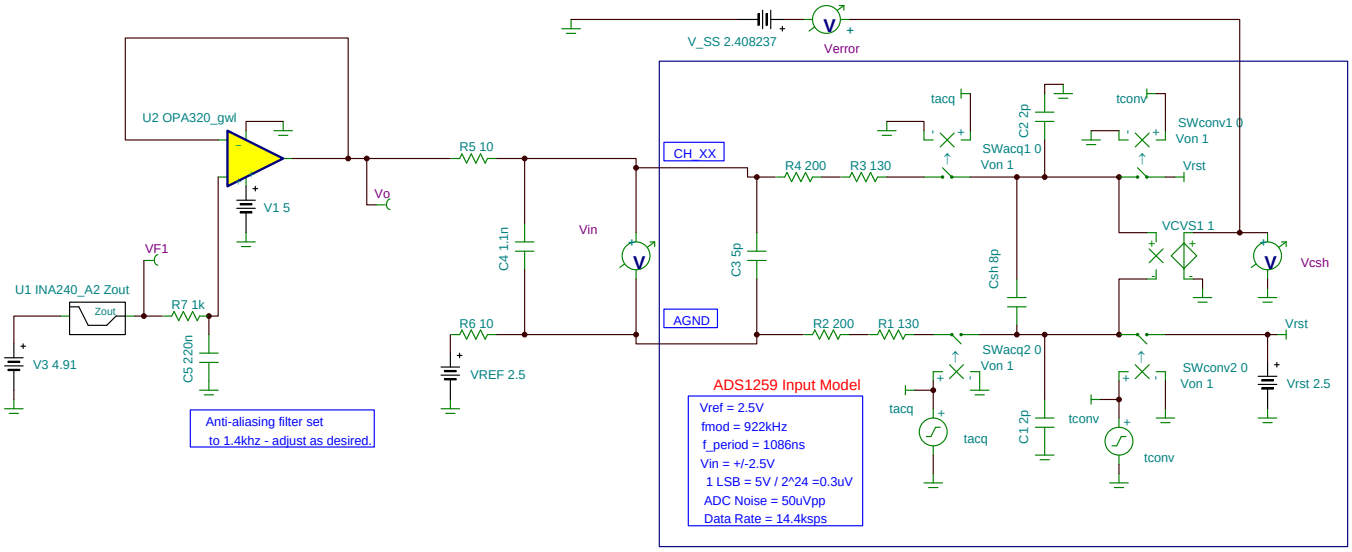

Figure 15. INA240 Output Connected to ADS1259 Through OPA320-Q1

The Vo and Vin signals on Figure 16 and Figure 17 are especially important to observe in these simulations. When connecting the INA240 to the ADS1259-Q1, Vo appears to behave like a sawtooth waveform, which indicates that the output signal is not sufficiently sampled because of the effects of impedance mismatch or a mismatch on acquisition timings. The effect on Vo is also a result of the RC charge bucket, which can not tolerate these mismatches and results in an error in sampling and holding times. Due to this behavior when sampling occurs, the sawtooth behavior of the Vo signal that interacts with the ADC samples different values instead of the correct values. The simulation in Figure 17 avoids this effect, where the Vo and Vin signals behave mostly like a square wave, which indicates a more precise sampling. Verror and tacq are also much lower when the buffer amplifier has been connected.

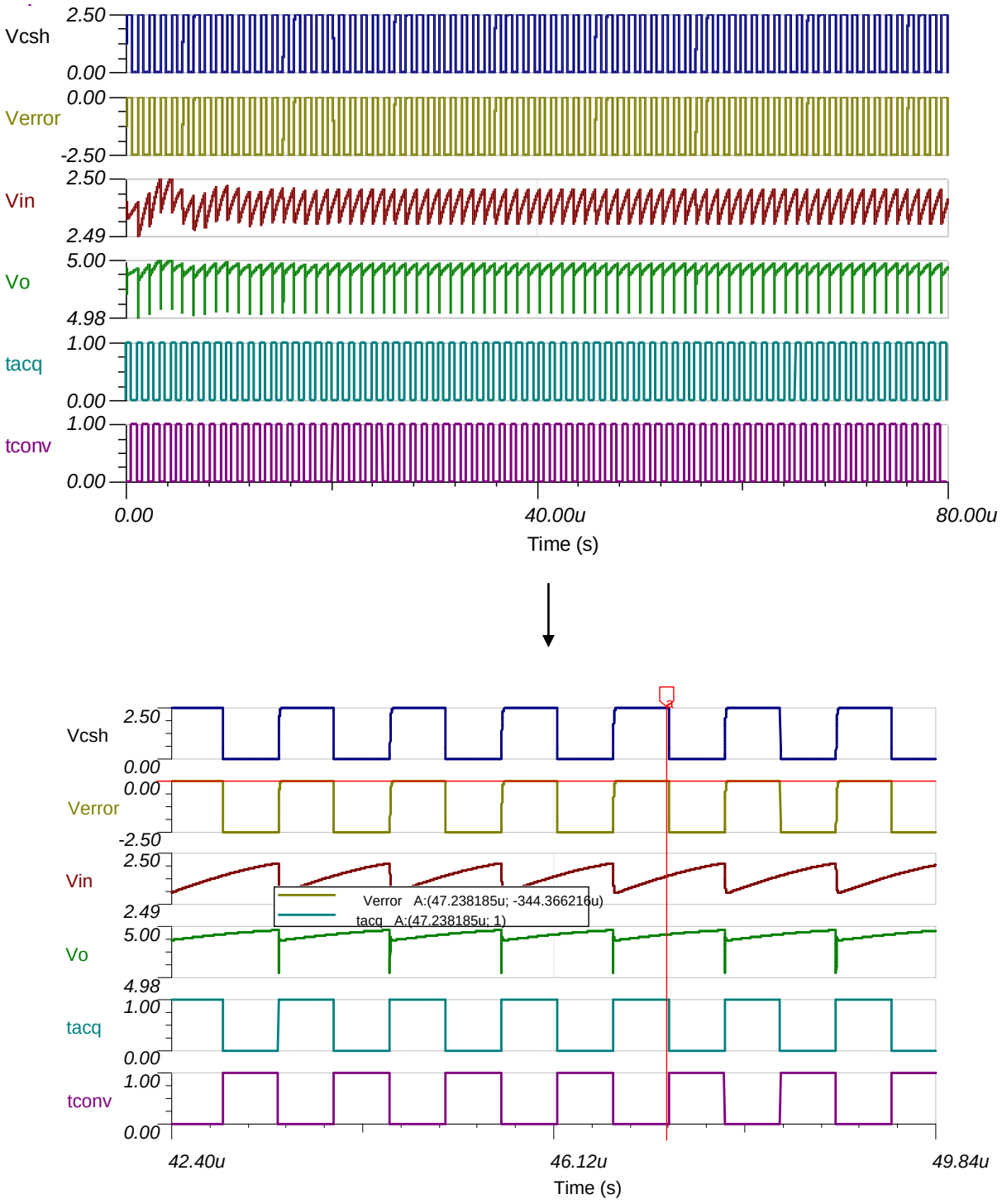

Figure 16. Voltage Signal Levels When INA240 Output is Directly Connected to ADS1259-Q1

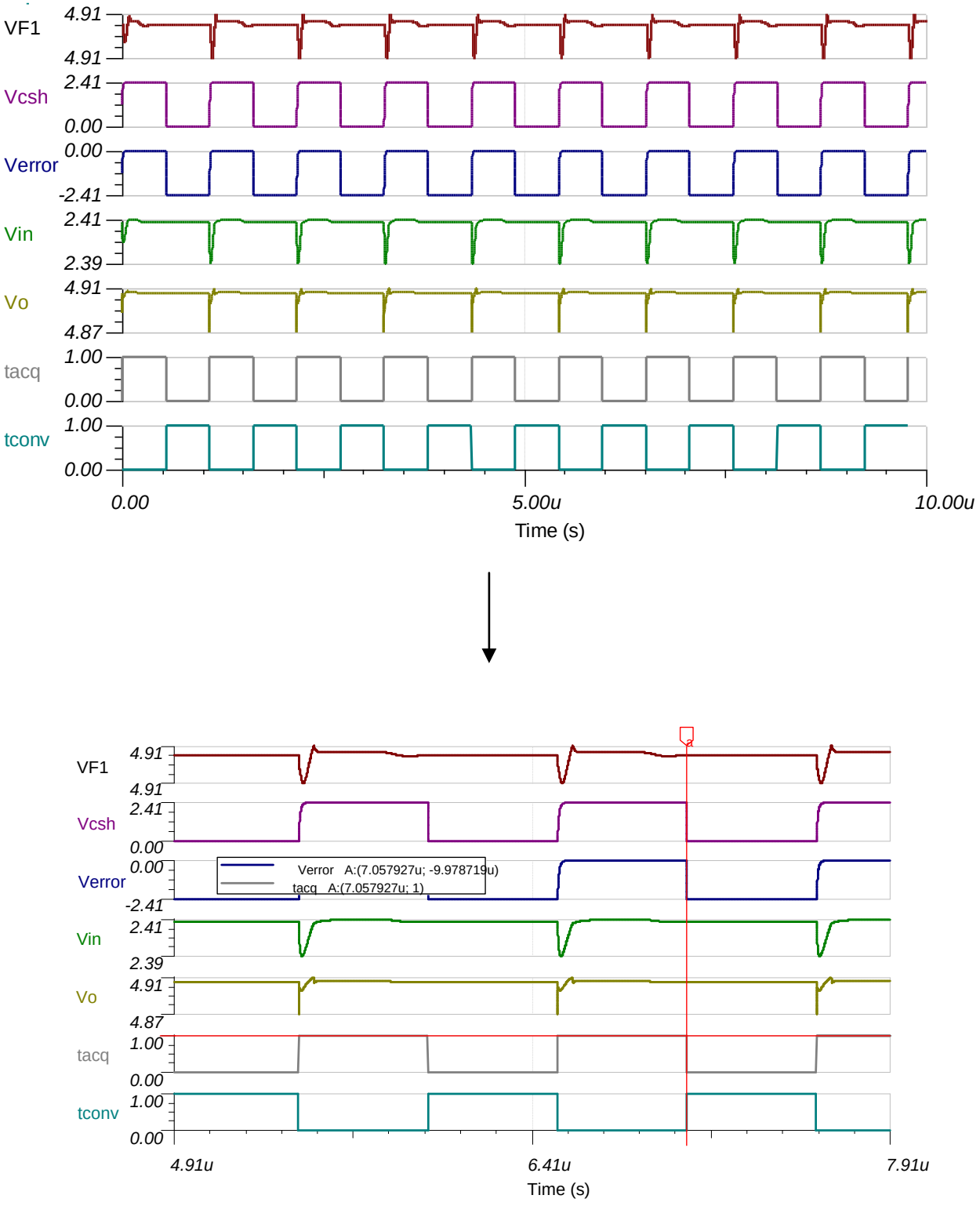

Figure 17. Voltage Signal Levels When INA240 Output is Connected to ADS1259 Through OPA320-Q1

2.3.3 Analog-to-Digital Conversion

The heart of the system is the ADS1259-Q1, which is a high-performance 24-bit ΔΣ ADC that is capable of obtaining a high resolution even at lower currents. This ADC offers a high-precision low-noise voltage reference. Due to the high-dynamics range and the bipolar input of the ADC, a passive AFE is possible, which avoids additional noise sources.

A 24-bit ADC is required because of the large current ranges and requirements on measurement accuracy over a large range span. A higher resolution ADC provides low quantization noise, which improves accuracy. An ADC internal reference is connected to the reference terminals of the INA240 device as well, which makes the total measurement shift there ratiometrically by reusing the voltage reference error. A differential signal is applied across the ADC input terminals from the INA240 output through the OPA320-Q1 buffer amplifier. The ADS1259-Q1 device can support up to 14.4 kSPS, which enables the user to capture the signal update rate quickly by increasing the system update rate. The ADS1259 has internal registers for calibration. Gain and offset registers scale the digital filter output to produce the final code value. On-command calibration corrects for system offset and gain errors. Figure 18 shows the ADC schematics.

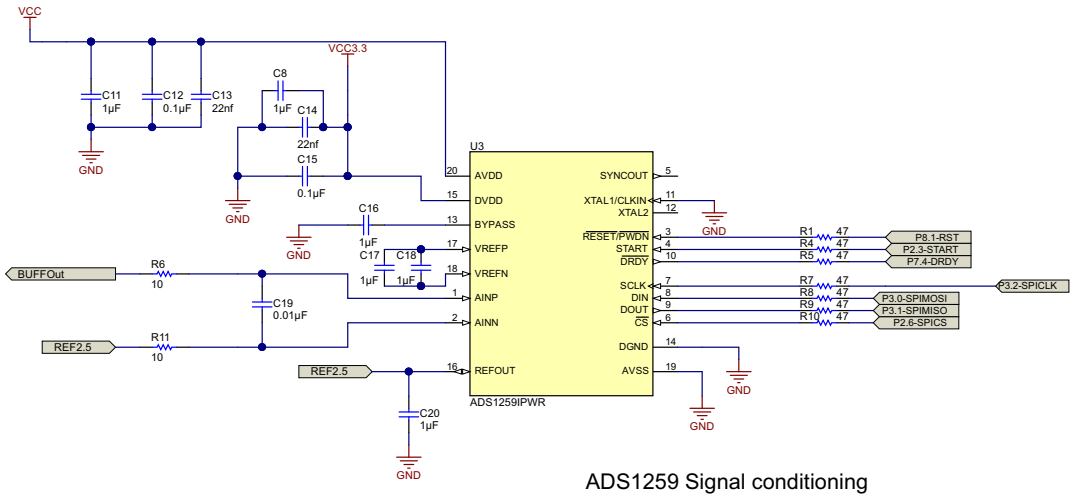

ADS1259 Signal conditioning

Figure 18. ADS1259-Q1 Schematic

2.3.4 Shunt Temperature Measurement

Use a silicon temperature sensor to compensate for temperature and linearity effects in the system. A temperature sensor measure the real-time temperature of the shunt and adjusts the measurement error based on the shunt temperature. Temperature sensor information is important for making error estimations of the system because resistors typically vary a lot with temperature, as do the current shunts. Shunt manufacturers provide the resistance change with respect to shunt variations. Take this information into consideration when calculating the resistance change. Measure the temperature of the shunt. Figure 19 shows the shunt temperature schematics. The temperature of the shunt increases in two cases:

- Higher currents indicates a higher power dissipation, which indicates a higher temperature across the shunt
- Ambient temperature (depends on the shunt location)

For this reference design, attach an LMT01 temperature sensor to the shunt and monitor the temperature of the shunt to compensate for the errors in current measurements. The voltage measured across the temperature sensor (LMT01-Q1) is proportional to the temperature of the shunt element, which is determined by the characteristic equation of LMT01-Q1. An output resistor at 100 K, along with the transistor level-shifter configuration, results in output pulses in the range of 3.3 V. These pulses are then sent to the MCU general-purpose input/output pins (GPIO) pins. Use the counter to count the number of pulses, which should be proportional to the temperature.

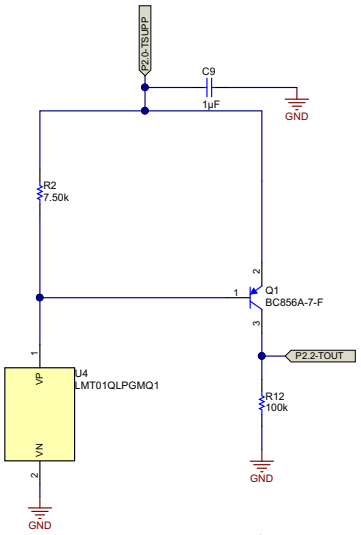

Temperature Sensor

Figure 19. Temperature Sensor Schematic

2.3.5 System Noise Estimation

Noise estimation plays a very important role in current sensors, especially when measuring lower currents where the noise is large because of the larger span of currents. When the current is lower, voltages across the shunt are in the range of µV. When the noise occurs in the µV range, then a signal dominates the noise, which results in a very noisy output. An estimate of the system noise helps to gather an understanding of how accurately the user can measure the lower currents. Figure 20 shows the contributors for system noise. These noise sources have all been vector summed to estimate the final noise performance of a system. Out of all the noise sources, the main contributors of these are as follows:

- Sensor noise (shunt noise)
- Amplifier noise (INA240 noise)
- ΔΣ ADC noise (ADS1259-Q1)
- Layout noise

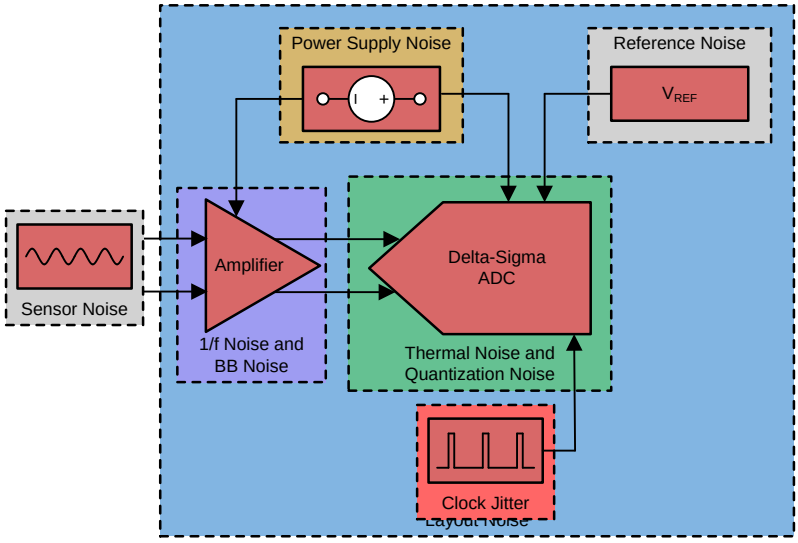

Figure 20. Current Sensor System Noise Sources

2.3.5.1 Sensor Noise (Shunt Noise)

This reference design uses a 37.5-µΩ shunt from Isabellenhütte Heusler GmbH & Co. KG, which has a tolerance of 5%. Figure 21 shows the resistance change with respect to temperature variation. Use temperature and linearity compensation algorithms to eliminate this error.

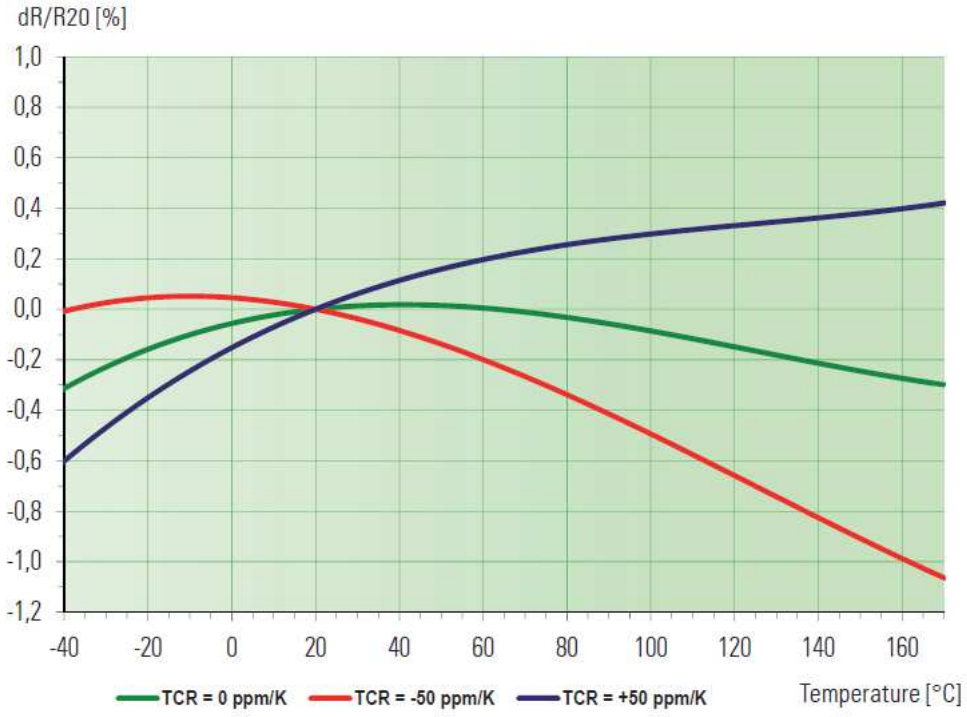

Figure 21. Resistance Change With Respect to Temperature Variations

NOTE: The temperature effect of the shunt has not been taken into account for the system noise calculations performed in the following subsections.

2.3.5.2 Amplifier Noise

The amplifier has broadband and 1/f noise. The amplification of this noise is performed with respect to the gain because the noise is multiplied by the gain. The ADC samples this noise, which allows the amplifier to affect the output code result. The input referred noise of an amplifier is the major contributor of noise in the system. The input amplifier used in this reference design is the INA240 current shunt monitor. The INA240 is operated at a gain of 50 V/V. Figure 22 shows a plot of the input referred noise density and Table 3 shows the specifications from the ADS1259-Q1 data sheet.

$$\text{Input Referred Noise (ADC Data Sheet)} = 40\ \text{nV}\sqrt{\text{Hz}} \quad (2)$$

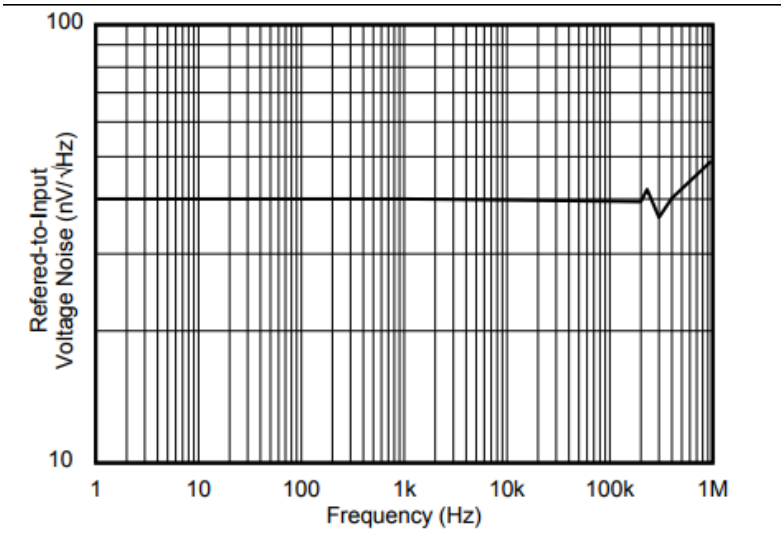

Figure 22. Input Referred Noise

Table 3. Voltage Noise Density From ADS1259-Q1 Data Sheet

PARAMETER		TEST CONDITIONS	MIN	TYP	MAX	UNIT
FREQUENCY RESPONSE						
BW	Bandwidth	All gains, –3-dB bandwidth	—	400	—	kHz
		All gains, 2% THD+N[1]	—	100	—	
	Settling time – output settles to 0.5% of final value	INA240A1	—	9.6	—	µs
		INA240A4	—	9.8	—	
SR	Slew rate		—	2	—	V/µs
NOISE (INPUT REFERRED)						
	Voltage noise density		—	40	—	nV√Hz

(1) Excludes the internal reference error.

Figure 22 shows that, throughout the frequency change, the input referred noise density remains constant at 40 μV_{RMS}/root Hz.

Assume a worst-case scenario for the noise calculations, where the sampling rate is 14.4 kSPS, the chosen filter type is sinc[1], and the calculated effective noise bandwidth (ENBW) is 3269.4 Hz (see Section 2.3.5.3 for ENBW calculation). The following Equation 3 shows the amplifier noise calculations, where an ENBW of 3269.4-kHz V_{RMS} results in 2.28 µV. The selected gain configuration for the INA240 is 50 V/V, which indicates that the total amplifier noise is 114 μV_{RMS}.

$$V_{RMS}\left(\text{Amplifier}\right) = \frac{40\ \text{nV}}{\sqrt{\text{Hz}}} \times \sqrt{3269.4\ \text{Hz}}$$

$$\text{Amplifier Noise} = 2.28 \times 50\ \text{V/V}\ \mu V_{RMS}$$

$$\text{Amplifier Noise} = 114\ \mu V_{RMS} \quad (3)$$

NOTE: All the noise calculations are performed for a worst-case scenario, which is specified at 14.4 kSPS. Improve the noise performance by reducing the sampling rate.

2.3.5.3 ADC Noise

The ADC has a certain amount of inherent noise. The two main types of noise in a ADC are thermal and quantization noise. The ADS1259-Q1 has a resolution of 24 bits, which implies that the thermal noise dominates the quantization noise because, when the resolution is high, the ADC has sufficient levels for the approximation values.

Table 4 shows the typical noise data versus the data rate and digital filter of the ADS1259-Q1. The ADC noise varies with the data rate and resolution; as the data rate increases the ADC noise increases and vice versa. Running the ADC at an optimal rate is preferable to obtain better accuracy at a higher data rate. For the ADC noise calculations, this reference design assumes that the user is running the ADC at 14400 SPS and using a sinc[1] digital filter.

Table 4. ADS1259-Q1 Inside Digital Filters

DATA RATE (SPS)	SAMPLE SIZE[(1)]	SINC[1] DIGITAL FILTER				SINC[2] DIGITAL FILTER			
		NOISE (μV_{RMS})	NOISE (μV_{PP})	ENOB (RMS)	NOISE-FREE BITS	NOISE (μV_{RMS})	NOISE (μV_{PP})	ENOB (RMS)	NOISE-FREE BITS
10	128	0.5	1.8	23.3	21.4	0.45	1.6	23.4	21.6
16.6	256	0.55	2.4	23.1	21.0	0.5	2	23.3	21.3
50	512	0.65	3.5	22.9	20.4	0.6	3	23.0	20.7
60	512	0.7	4	22.8	20.3	0.65	3.5	22.9	20.4
400	4096	1.4	9.5	21.8	19.0	1.2	8.3	22.0	19.2
1200	8192	2.3	17	21.1	18.2	2	14	21.3	18.4
3600	8192	3.9	32	20.3	17.3	3.4	27	20.5	17.5
14400	8192	6.2	20	19.6	16.6		[(2)][(2)]	[(2)]	[(2)]

(1) Data sample sizes used for analysis.
(2) Same as Sinc[1] mode.

Knowing the effective noise bandwidth of the system is essential for the user to calculate the ADC noise. Figure 23 shows that the ADC terminals are shorted. Using this arrangement, calculate the effective number of bits (ENOB) to calculate the RMS noise of the ADC.

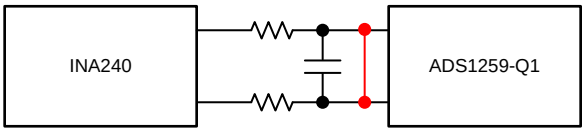

Figure 23. Shorted ADC Input Terminals

The measured ENOB from the ADC output is ENOB = 19 (at a 14.4-kSPS data rate). The full-scale input range of the ADC is FSR = 5 V (–2.5 V to +2.5 V).

The following Equation 4 shows a possible way of calculating the RMS noise of the ADC using known values of the ENOB and FSR. As the equation shows, the RMS noise of the ADC is 9.6 μV_{RMS}.

$$\text{ENOB} = \frac{\ln \frac{\text{FSR}}{\text{RMS Noise}}}{\ln 2}$$

$$19 = \frac{\ln \frac{5}{\text{RMS Noise (thermal)}}}{\ln 2}$$

$$\text{RMS Noise (thermal)} = 9.6\ \mu\text{VRMS} \tag{4}$$

Along with the RMS noise, the ADC is also responsible for other noises such as input noise and reference noise.

The input noise = 0.5 μV_{RMS} (input is –50 mV to +50 mV). The reference noise = 0.4 μV_{RMS} (2.5-V internal reference; the reference is ratiometric to the input).

Other noise sources are also present; however, compared to these three primary sources of noise, they are insignificant and can be considered negligible. Equation 5 and Equation 6 show a calculation of the total ADC noise. After considering all the ADC noise, the total vectored sum of ADC noises is determined to be 6.531 μV_{RMS}.

$$\text{Total ADC Noise} = \sqrt{\text{RMS Noise (thermal)}^2 + \text{Input Noise}^2 + \text{Reference Noise}^2} \quad (5)$$

$$\text{Total ADC Noise} = 6.531\,\mu\text{VRMS} \quad (6)$$

The effective noise bandwidth is the bandwidth of an entire system, which the user can determine by considering the noise sources.

The amplifier bandwidth = 400 kHz.

Table 5 shows that, at a sampling rate of 14.4 kSPS and using the sinc[1] filter, the resulting bandwidth is –3 db at 2930 Hz. The effective noise bandwidth (ADC plus the antialiasing filter) = 3269.4 Hz

Table 5. Sinc Filter –3-db Bandwidth

DATA RATE (SPS)	FIRST NOTCH (Hz)	–3-dB BANDWIDTH (Hz)	
		SINC[1]	SINC[2]
10[(1)]	10	4.3	3.1
16.6[(2)]	16.6	7.3	5.2
50	50	22	13
60	60	27	19
400	400	177	127
1200	1200	525	380
3600	3600	1440	1100
14400	14400	2930	See[(3)]

(1) Notch at 50 Hz and 60 Hz.
(2) Notch at 50 Hz.
(3) Same as Sinc[1].

2.3.5.4 PCB Layout Noise

The PCB layout noise plays an important role when measuring the noise for the high-speed, high-resolution ADC. Figure 24 labels the pertinent PCB layout guidelines.

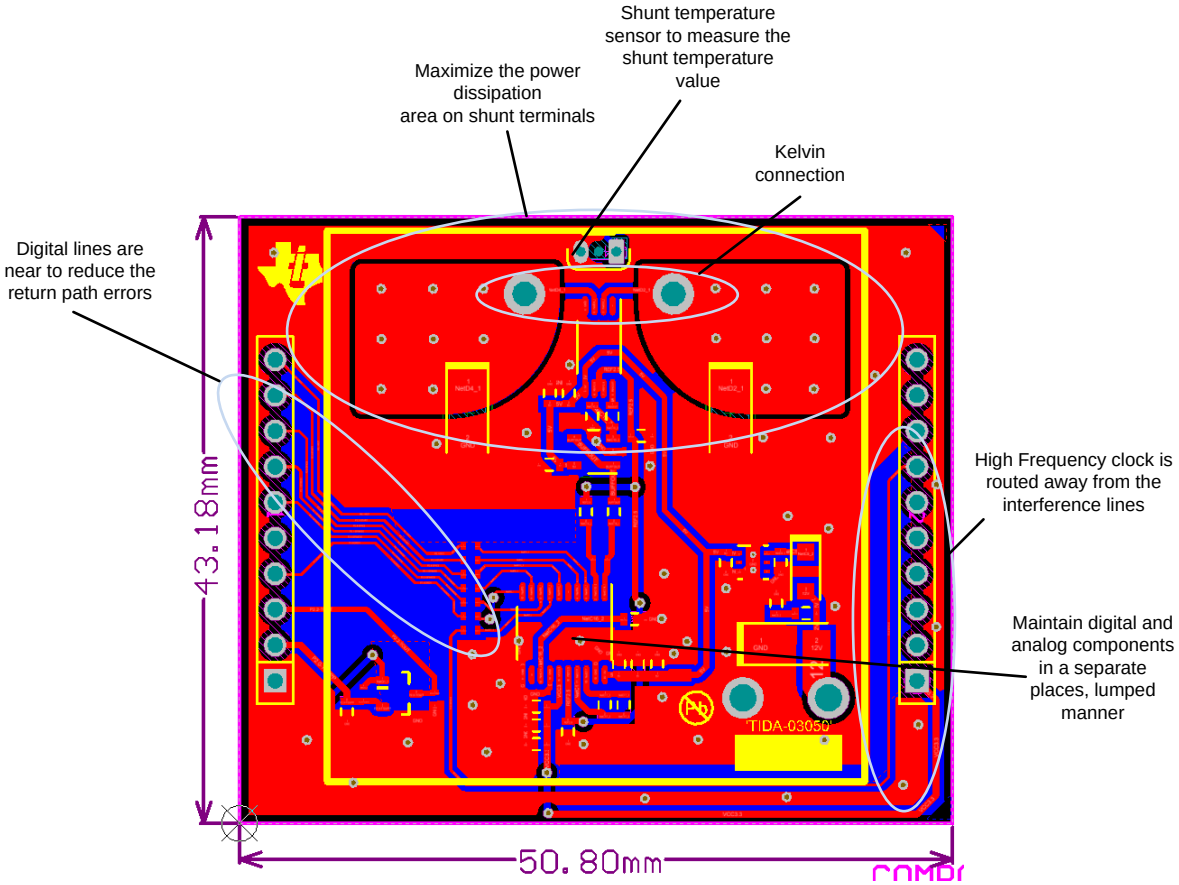

Figure 24. PCB Layout Guidelines

2.3.5.5 Total System Noise Estimation

The total system noise is the vector sum of all the major noise sources in the system. The following Equation 7 describes the total system noise calculation. The total system noise of the system is 114.186 μV_{RMS}.

$$\text{Total System Noise} = \sqrt{\text{Amplifier Noise}^2 + \text{ADC Noise}^2}$$

$$\text{Total System Noise} = 6.92\ \mu V_{RMS}$$

$$\text{Total System Noise} = 114.186\ \mu V_{RMS} \quad (7)$$

3 Getting Started Hardware and Software

In typical current shunt designs, ±1300 A of current passes through the shunt and the resulting voltage is provided to the signal conditioning unit. In this reference design, instead of directly passing ±1300 A through the shunt, the voltage across the shunt is emulated using a precision source meter. First calibrate the device, then perform the basic functional tests proceeded by temperature variation tests. The main testing objective is to prove that the current sensor maintains good accuracy over the entire temperature range.

The following equipment is required for the initial board setup:

- TIDA-03050 PCB
- MSP430F5529 LaunchPad™
- PC (with the Python Virtual Instrument Software Architecture (VISA) environment installed)
- 12-V battery or power supply
- HP 3458A 8½ digit multimeter (preferably)
- Keysight 34410A 6½ digit multimeter (preferably)
- Keysight source meter B2912A (preferably)

3.1 Hardware Connections

Connect the hardware as follows:

1. Connect the circuit as described in Figure 25.
2. Connect the 12-V power supply or battery.
3. Connect the input differential wires to the Keysight source meter B2912A and to the HP 3458A 8½ digit multimeter to measure how much voltage is applied through the source meter.
4. Apply the 3.3-V serial peripheral interface (SPI) pins from the MSP430™ LaunchPad to the TIDA-03050 board to form a BoosterPack™ Plug-in Module configuration.
5. Connect the MSP430 LaunchPad USB to the PC through a USB cable and acquire the serial information through a Python-developed program.

Figure 25 shows the board test setup.

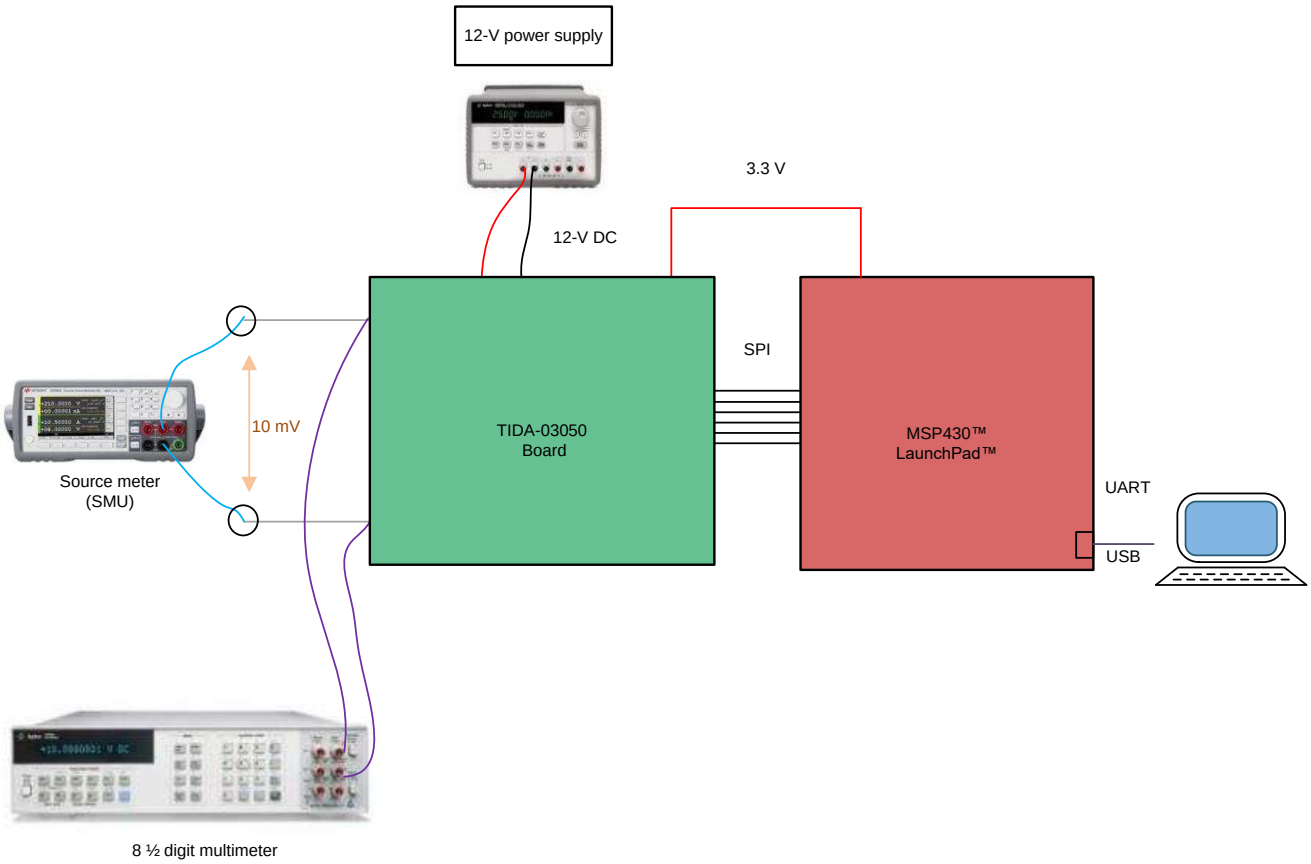

Figure 25. TIDA-03050 Board Test Setup

3.2 Software

The software setup is as follows:

1. Install the provided binary file in the Code Composer Studio™ (CCS) integrated development environment.
2. Debug and run the program.
3. Open hyperterminal or a Python environment to acquire the 24-bit digital data through a USB cable.

4 Testing and Results

This section shows the test results of the TIDA-03050 reference design. The test software has been written on the MSP430F5529 LaunchPad (shown in Figure 26). The TIDA-03050 board transmits the information to the MSP430F5529 through SPI. A separate capture input of the MSP430 counts the pulses from the LMT01, which acts as the temperature sensor for the shunt resistor temperature measurements. The user interface has been written in Python in such a way to automate the equipment and retrieve the bunch of values for a variety of inputs. The user can set the register configuration different settings using CCS.

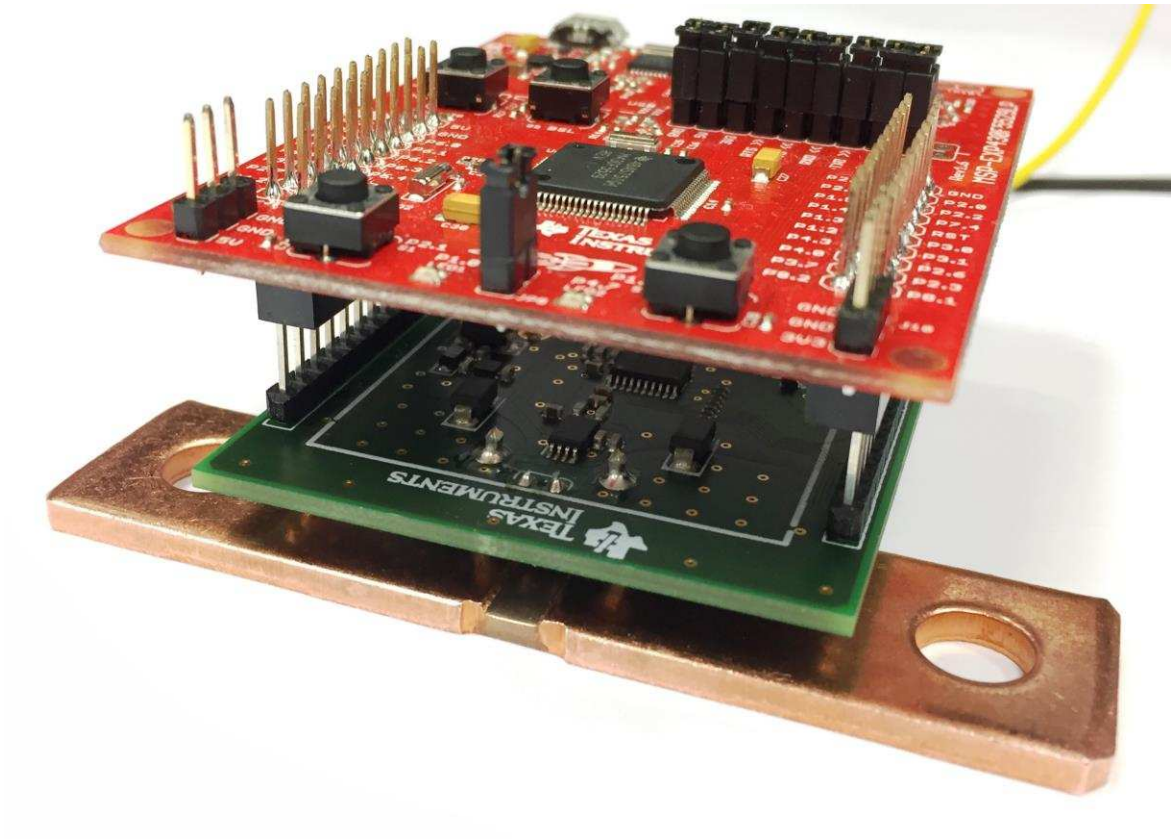

Figure 26. TIDA-03050 Board With MSP430F5529 LaunchPad™

The user interface is developed by an automated test environment (ATE) and the script is written in Python and connects the TIDA-03050 board with the ATE. The raw test results are written to a .csv file for further data processing. The previous Figure 25 shows the connection of the test equipment.

4.1 Measuring Shunt Value

Apply 30 A of current by setting the load power to 30 W. Measure the voltage across the shunt: V = I × R, which means that R = V / I. The variable I is the applied current from the power supply and V is the measured voltage across the terminals of the shunt. Using these two known values, the designer can calculate the resistance using the R = V / I formula. The resistance value is the voltage divided by current. Figure 27 shows the setup diagram for measuring the shunt value.

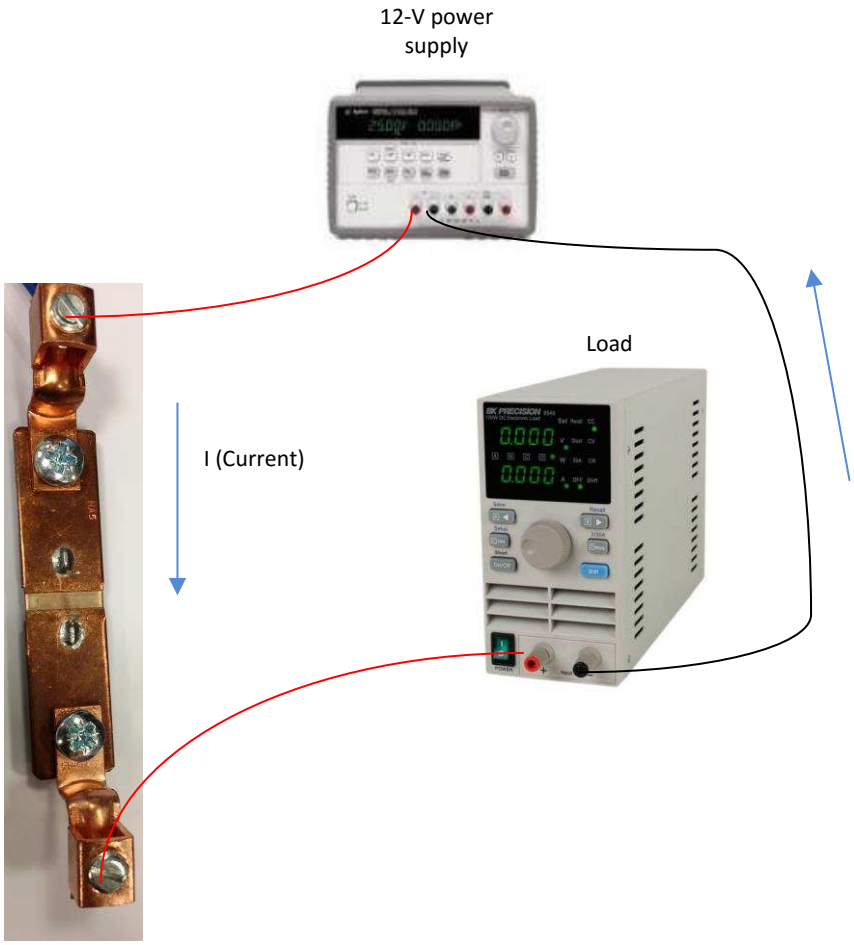

Figure 27. Shunt Value Measurement

4.2 Functionality Testing

The functional test includes verifying the device functionality for accuracy and bandwidth. The user can configure the INA240 and ADS1259-Q1 devices in a variety of configurations such as data rate, resolution, gain, reference, and so forth, depending on which particular configuration is required. The following subsections describe the test results for each scenario.

The INA240 and ADS1259 devices have been configured as such for the following test results:

1. Power supply set to +12-V DC (LDO); ADS1259 and INA240 receive 5 V.
2. Shunt (37.5 µΩ)
3. Current shunt monitor (INA240):
   a. Gain 50 V/V
   b. Supply 5 V
   c. Reference 2.5 V
   d. Kelvin connection between INA240 and shunt (37.5 µΩ)

4. ADC (ADS1259):
   a. Internal reference 2.5 V
   b. Supply 5 V
   c. SPS (10, 16, 50, 60, 400, 1200, 3600, 14400)
   d. Sinc[1] filter
5. Internal oscillator
6. Temperature –40°C to 125°C

By considering the preceding parameters, the test results sections are classified in the following two categories:

1. Samples distribution for different data rates
2. Accuracy estimation
   a. 25°C temperature results
   b. 50°C temperature results

4.2.1 Samples Distribution for Different Data Rates

The ADS1259-Q1 supports the transmission of eight different data rates (14.4 kSPS, 3.6 kSPS, 400 SPS, 60 SPS, 1200 SPS, 50 SPS, 16.6 SPS, and 10 SPS). To estimate the noise performance at different data rates, short two inputs together to the ground and take 128 samples for each set of data. Connect the setup as Figure 28 shows.

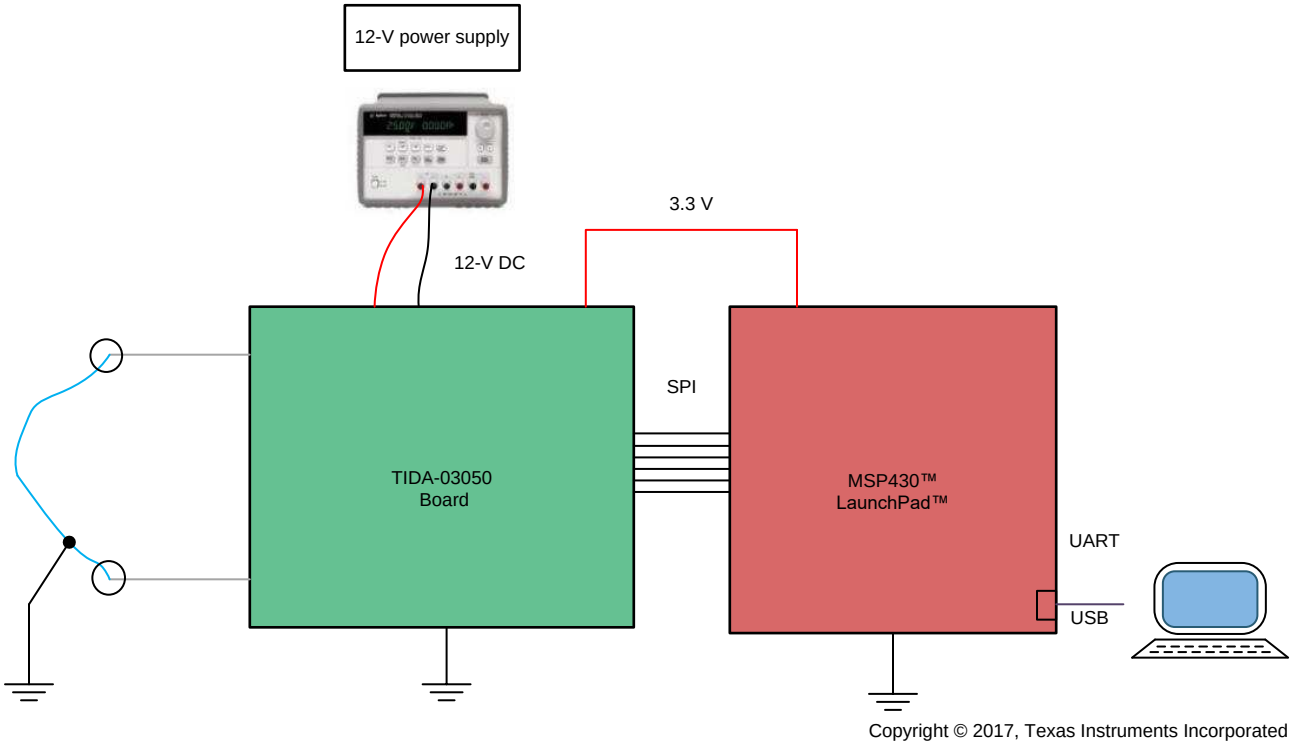

Figure 28. Input Terminals Shorted to Ground

Figure 29 through Figure 36 show the histograms for signal samples with different samples per second at temperatures of 25°C. Each figure shows the mean and standard deviation of samples to estimate how much deviation the measurement has for a particular data rate. These histograms show that, as the data rate decreases, the sample distribution is much narrower and the standard deviation is also quite less.

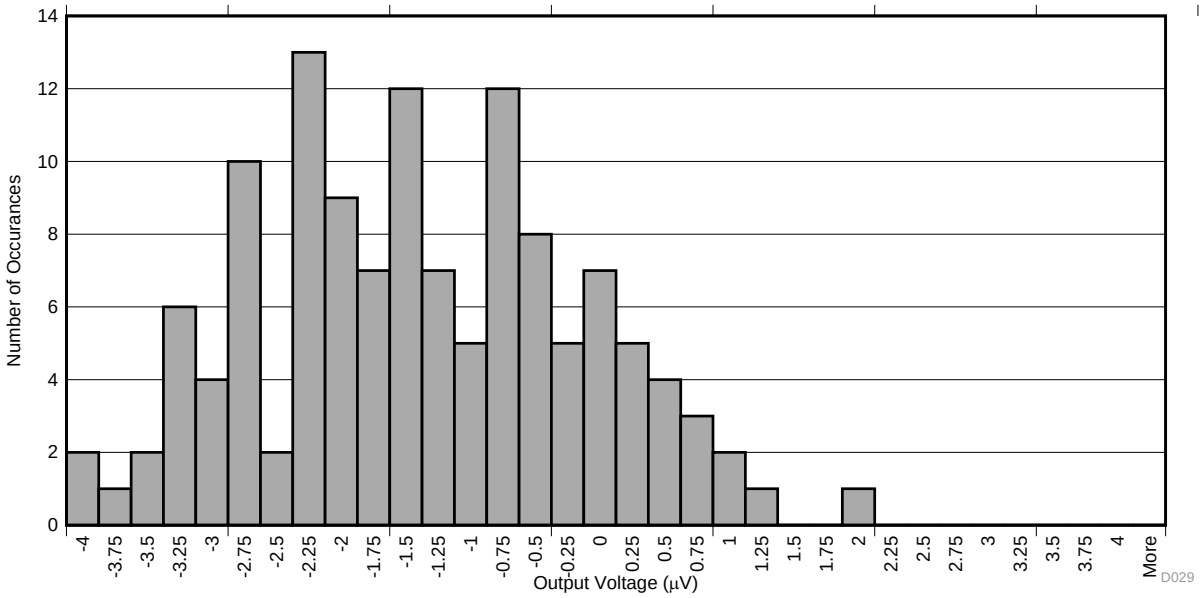

14 kSPS
Mean: –1.5247147530317 µV
STD: 1.267567506 µV

Figure 29. Distribution at 25°C and 14.4 kSPS

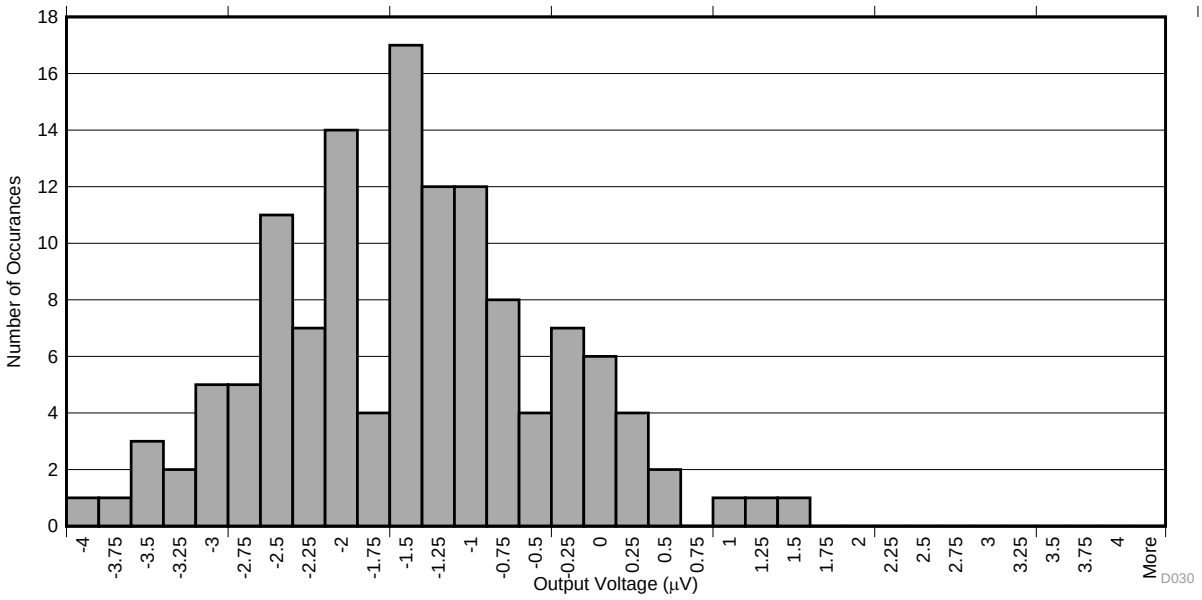

3600 SPS
Mean: –1.6037374734879 µV
STD: 1.07485239 µV

Figure 30. Distribution at 25°C and 3.6 kSPS

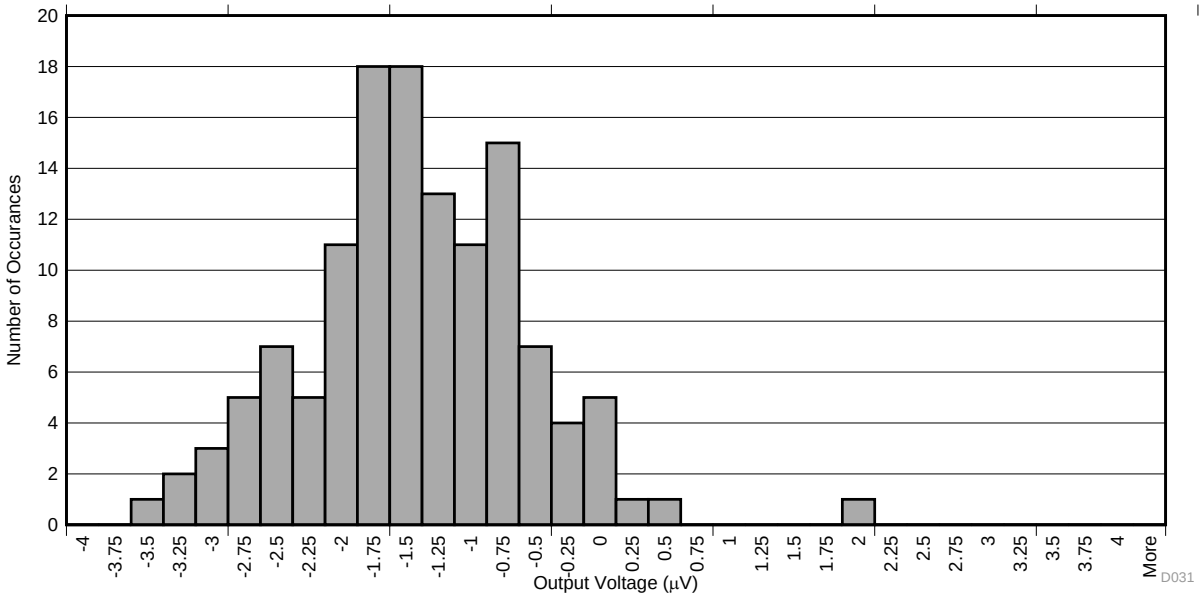

1200 SPS
Mean: –1.5484169125557 µV
STD: 0.502646572 µV

Figure 31. Distribution at 25°C and 1200 SPS

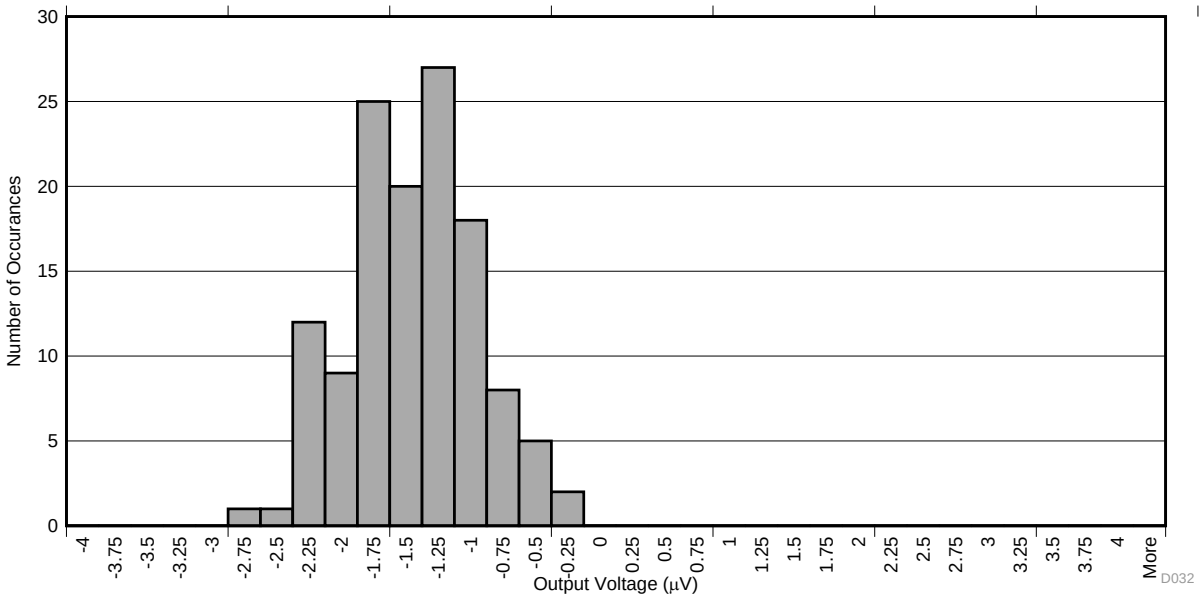

400 SPS
Mean: –1.5683061494602 µV
STD: 0.50366757 µV

Figure 32. Distribution at 25°C and 400 SPS

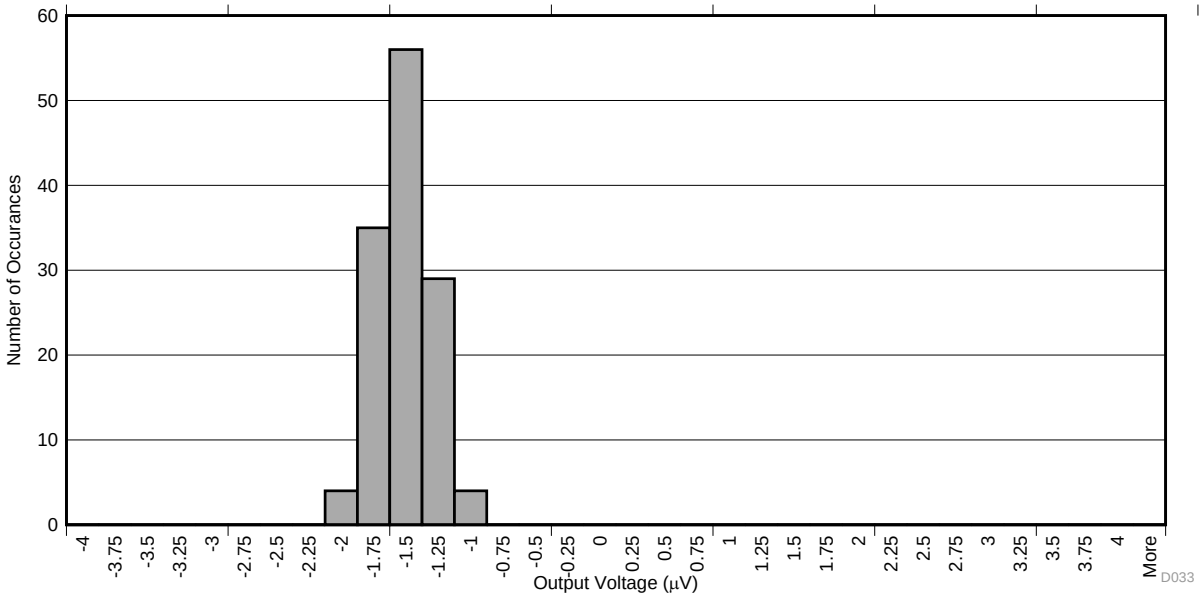

60 SPS
Mean: –1.6446188678892 µV
STD: 0.197507312 µV

Figure 33. Distribution at 25°C and 60 SPS

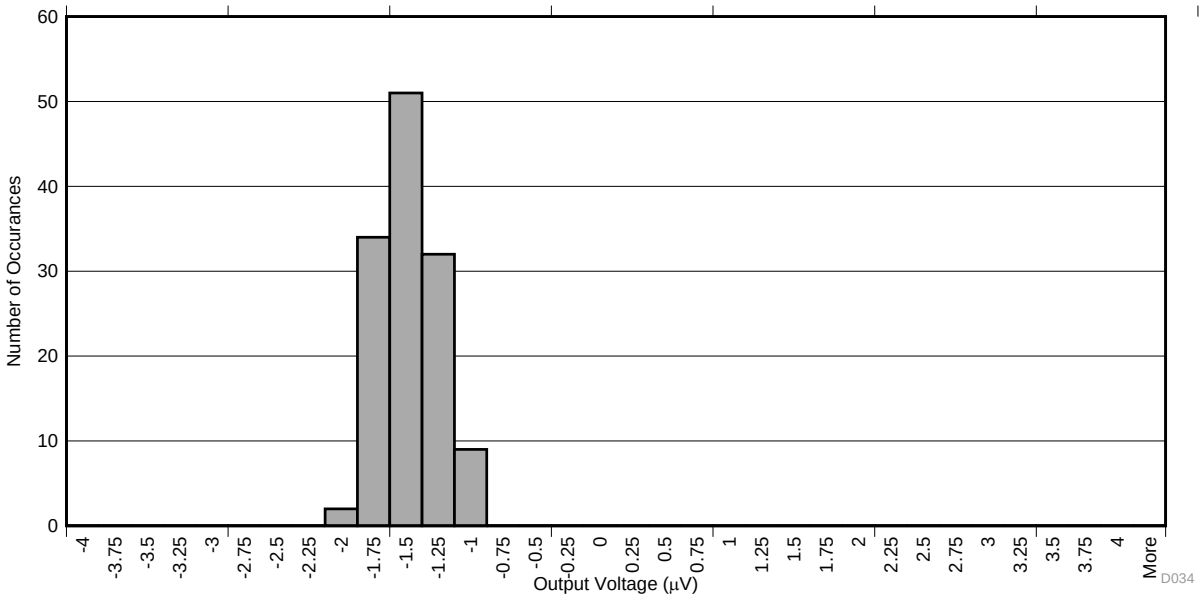

50 SPS
Mean: –1.6035977751017 µV
STD: 0.20798493 µV

Figure 34. Distribution at 25°C and 50 SPS

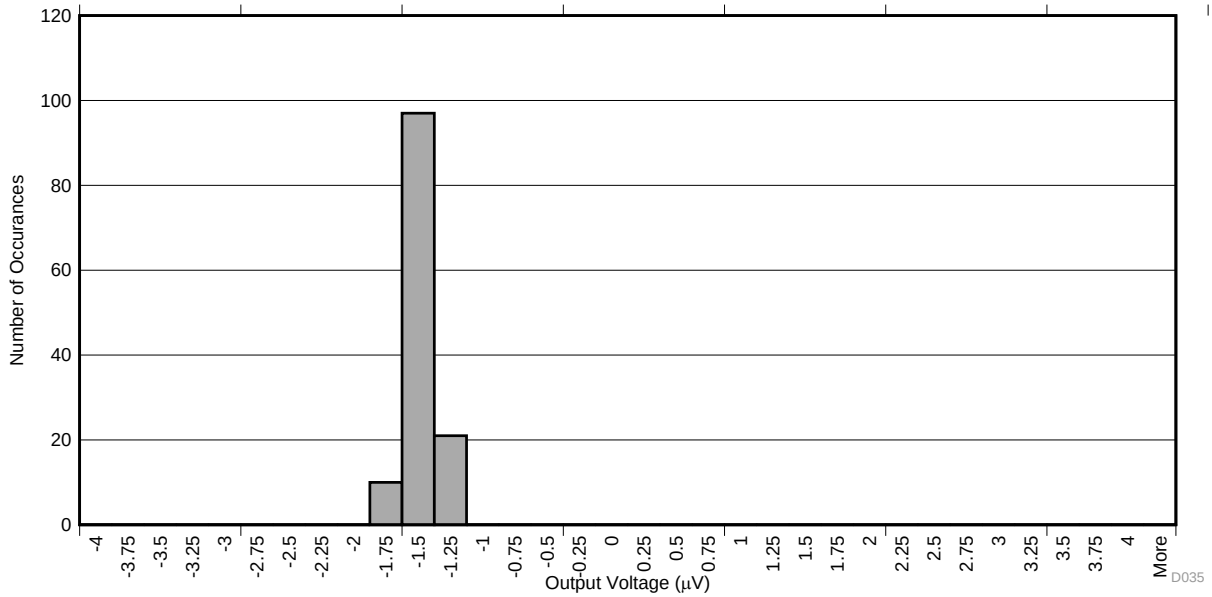

16.6 SPS
Mean: –1.6042962670326 µV
STD: 0.106338821 µV

Figure 35. Distribution at 25°C and 16.6 SPS

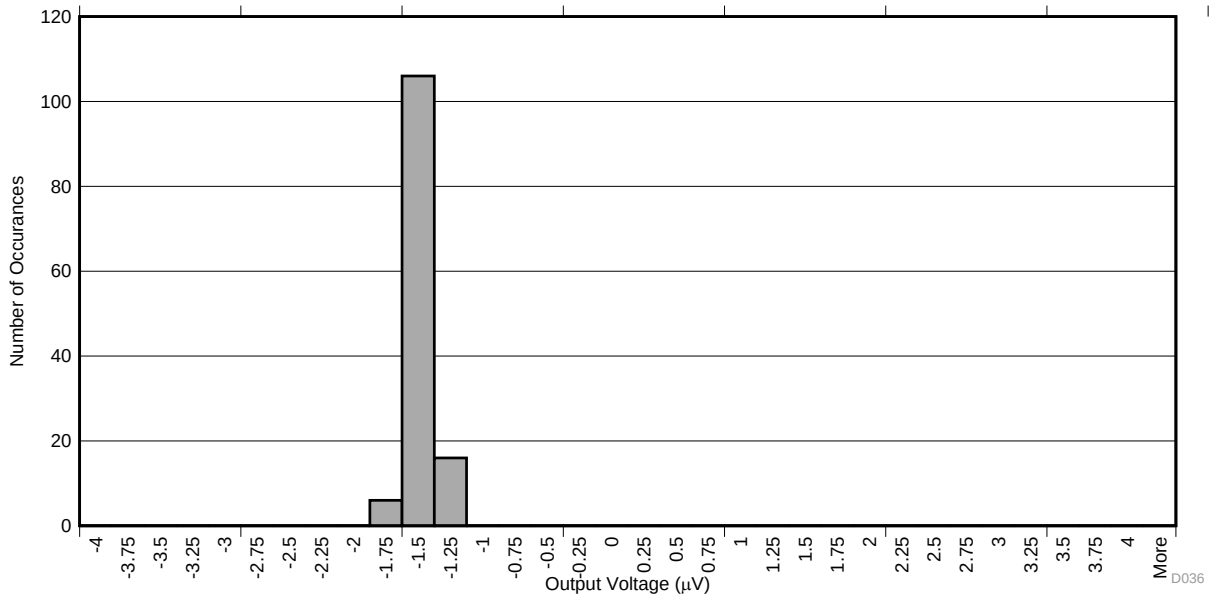

10 SPS
Mean: –1.5986617654562 µV
STD: 0.090570069 µV

Figure 36. Distribution at 25°C and 10 SPS

The standard deviation is noticeably higher when the sampling rate is high and the standard deviation is noticeably lower when the sampling rates are lower. This relationship implies that the ADC must be driven at the optimum data rate to obtain high accuracy. So a trade-off exists between the high sampling rate and the accuracy. When the bandwidth is more important, run the ADC at 14.4 kSPS. When the accuracy is more important, yet a reasonable bandwidth is still required, choose a 3.6-kSPS rate under normal circumstances. Implement different filters in the software to switch the data and obtain the best performance from the ADC.

4.2.2 System Accuracy Estimation

Sensor accuracy, especially when dealing with battery current sensors, is a critical factor to consider because it directly affects the BMS and its ability to accurately measure parameters such as pack voltage, charging and discharging current, individual cell voltages, battery disconnection in abnormal conditions, charge stored by each cell in a stack, operational status of system components to assist with functional safety, SOC, SOH, and SOF. These parameters all depend on the accuracy of the sensor inputs. The accuracy of a current sensor is important, especially at lower currents, for making very prompt decisions which increase system efficiency. Sensor accuracy is normally specified separately for lower and higher currents. Connect the setup as shown in Figure 37 to perform an accuracy estimation.

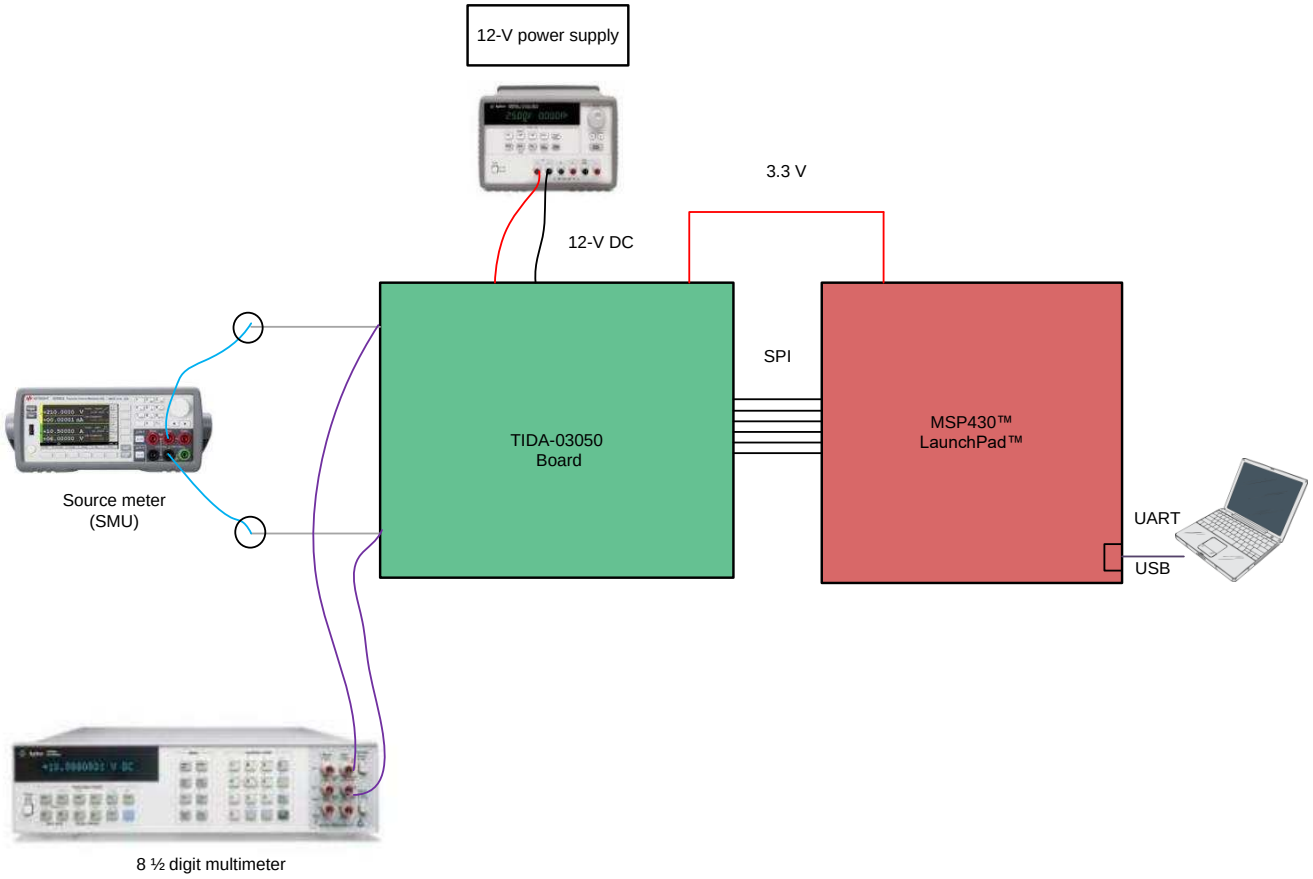

Figure 37. Accuracy Estimation Setup (ATE Setup)

To estimate the accuracy, this reference design used a Keithley source meter to emulate 1500 A. Use a source meter to apply an equivalent differential voltage for the 1500 A across two shunt terminals. To obtain the exact value of the applied source meter voltage, connect an 8½ digit multimeter to the INA240 terminals (this voltage is considered to be the input voltage). Calculate the output voltage using the following steps.

1. Set the data rate in CCS.
2. Import the program onto the LaunchPad and ADS1259-Q1 device.
3. Apply the voltage with the source meter.
4. Collect 128 samples of this applied voltage and average these values to the output voltage.
5. Use the ATE developed in Python to ensure that the complete equipment has been automated for the purpose of averaging these values.
6. 2000 samples are applied between –1300 A to 1300 A across the inputs with a 10-ms time difference and the outputs are recorded.
7. Offset calibration: Record the output when the input is zero and subtract all the values from this value.
8. Gain calibration: Take the maximum input divided by the maximum output and multiply each value with this ratio to the gain-calibrated value.
9. Conversion to current: The resistance value is calculated as described in Section 4.1. The ADS1259-Q1 output code is converted to equivalent voltage values. Calculate the current using these known resistance and voltage values.
10. Accuracy calculation: Estimate the full-scale accuracy (FSA) using the following formula in Equation 8:

$$\text{FS Accuracy} = \left(\text{Output Expected}\left(\text{V}\right) - \text{Output Measured}\left(\text{V}\right)\right) \times \frac{100}{\text{Output Span}} \quad (8)$$

11. Temperature measurement: The temperature sensor remains connected to the board and shunt to compensate for the temperature dependance on the current sensor. Perform temperature compensation by using the look-up tables provided by the shunt manufacturer. The selected Isabellahaute shunt specifies the resistance variation with respect to the temperature, this way the temperature sensor detects the 50.2°C for a 50°C absolute temperature and the result is calculated based on this value. Following the previous steps, the accuracy is calculated at 50°C. The user can observe that the accuracy moves to ±0.3 because the system is not compensated for the temperature stability. Using the compensation algorithm, the user can reduce the accuracy over the required temperature range.

The accuracy is estimated in two steps, one is set at 25°C and the other at 50°C.

- Figure 38 and Figure 39 show the results at 25°C and 3.6 kSPS and 14.4 kSPS, respectively. As the plots show, the accuracy at 3.6 kSPS is much better in comparison to 14.4 kSPS. The accuracy estimate is:
  - –100 A to +100 A: < 0.02% FSR and –1300 A to +1300 A: ±0.05% FSR *(at 3.6 kSPS)*
  - –100 A to +100 A: < 0.04% FSR and –1300 A to +1300 A: ±0.08% FSR *(at 14.4 kSPS)*
- Figure 40 and Figure 41 show the results at 50°C and 3.6 kSPS and 14.4 kSPS, respectively. As the plots show, the accuracy at 3.6 kSPS is much better in comparison to 14.4 kSPS. The accuracy estimate is:
  - –100 A to +100 A: < 0.05% FSR and –1300 A to +1300 A: ±0.24% FSR *(at 3.6 kSPS)*
  - –100 A to +100 A: < 0.1% FSR and –1300 A to +1300 A: ±0.3% FSR *(at 3.6 kSPS)*

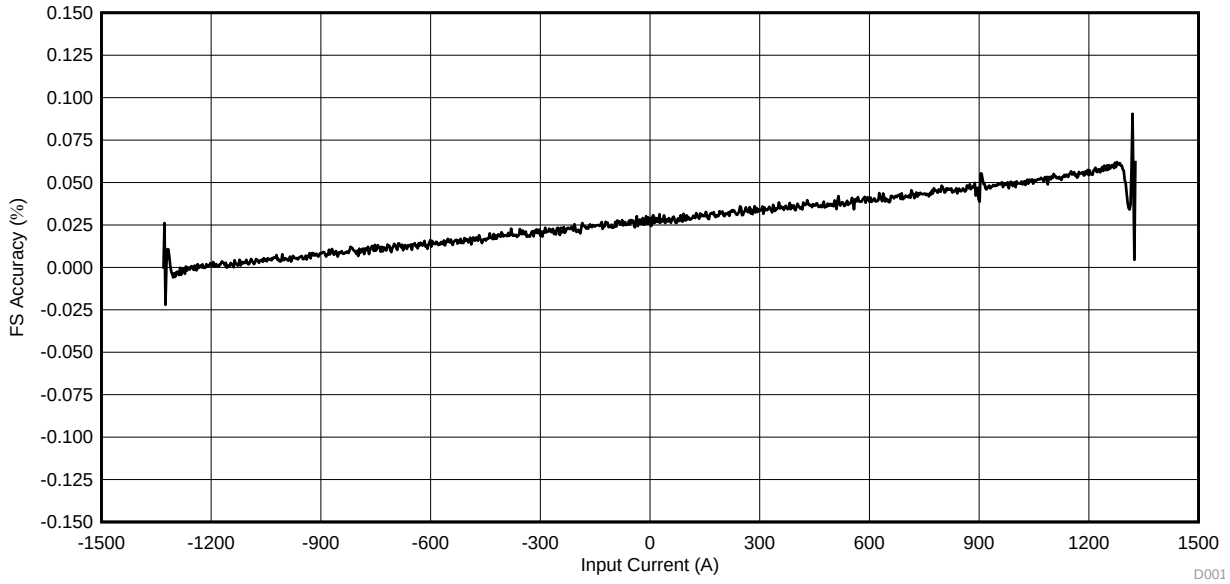

Figure 38. Full-Scale Accuracy in % at 25°C for –1500 A to +1500 A at 3.6 kSPS

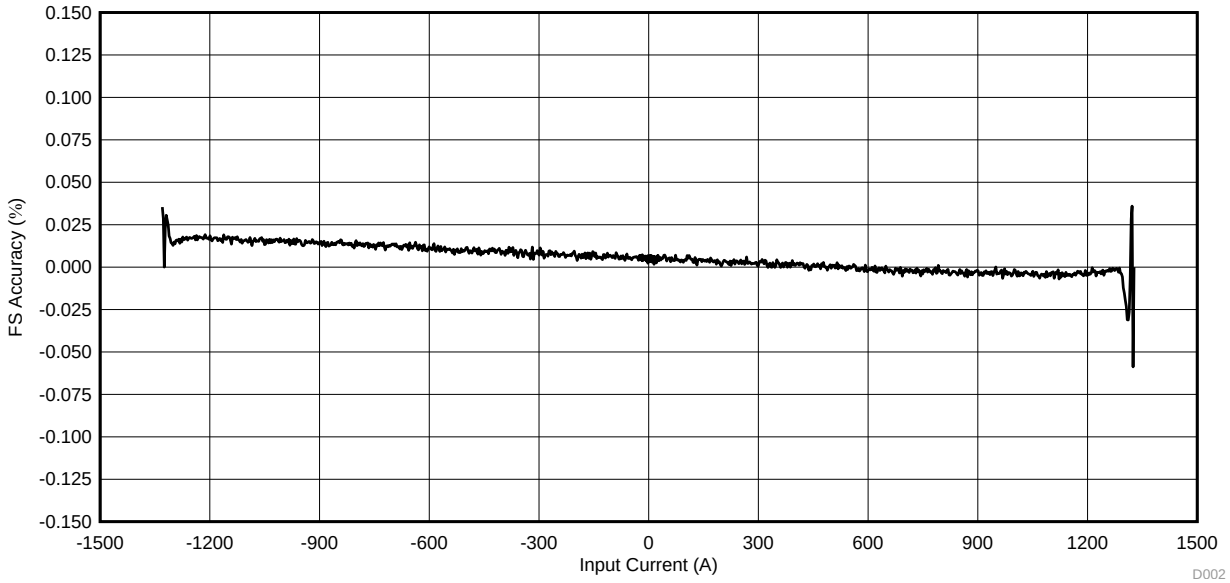

Figure 39. Full-Scale Accuracy in % at 25°C for –1500 A to +1500 A at 14.4 kSPS

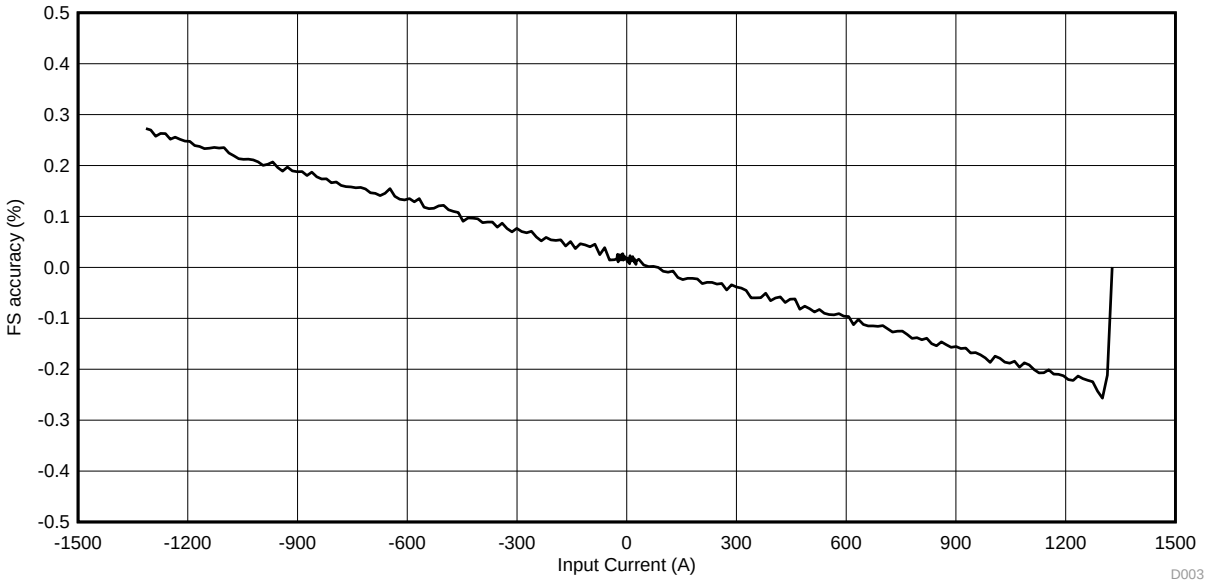

Figure 40. Full-Scale Accuracy in % at 50°C for –1500 A to +1500 A at 3.6 kSPS

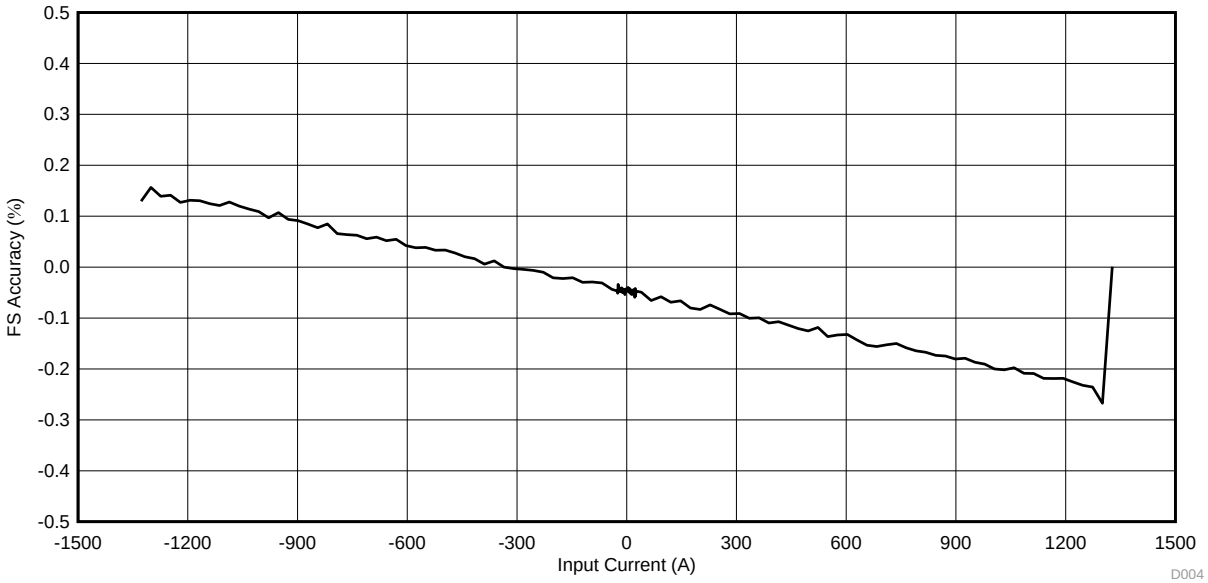

Figure 41. Full-Scale Accuracy in % at 50°C for –1500 A to +1500 A at 14.4 kSPS

5 Design Files

5.1 Schematics

To download the schematics, see the design files at TIDA-03050.

5.2 Bill of Materials

To download the bill of materials (BOM), see the design files at TIDA-03050.

5.3 PCB Layout Recommendations

Layout is one of the most critical factors when considering a current sensor design. Follow these guidelines when designing a current sensor solution.

5.3.1 Layout Prints

To download the layer plots, see the design files at TIDA-03050.

5.4 Altium Project

To download the Altium project files, see the design files at TIDA-03050.

5.5 Gerber Files

To download the Gerber files, see the design files at TIDA-03050.

5.6 Assembly Drawings

To download the assembly drawings, see the design files at TIDA-03050.

6 Software Files

To download the software files, see the design files at TIDA-03050.

7 Related Documentation

1. Texas Instruments, *Automotive Shunt-Based ±500-A Precision Current Sensing Reference Design*, TIDA-03040 Reference Design (TIDUCJ6)
2. Texas Instruments, *Current Shunt &Voltage Measurement Reference Design for EV/HEV Automotive Battery Monitoring*, TIPD201 Reference Design (TIDUA81)
3. Vishay.com, *Power Metal Strip® Battery Shunt Resistor W/ Molded Enclosure Very Low Value (50 μΩ, 100 μΩ, 125 μΩ, and 500 μΩ*, WSBM8518 (https://www.vishay.com/docs/31094/wsbm8518.pdf)
4. Isabellenhütte.de, *ISA-WELD® // PRECISION RESISTORS*, BAS // SIZE 8420 METRIC (http://www.isabellenhuette.de/fileadmin/content/praezisions-leistungswiderstaende/BAS.PDF)

7.1 Trademarks

8 Terminology

AFE— Analog front end

ATE— Automated test environment

BMS— Battery management system

CCS— Code Composer Studio™

CMRR— Common-mode rejection ratio

ENBW— Effective noise bandwidth

ENOB— Effective number of bits

EV— Electric vehicle

FSA— Full-scale accuracy

FSR— Full-scale range

GPIO— General-purpose input/output (pins)

HEV— Hybrid electric vehicle

LDO— Low-dropout regulator

RMS— Root mean square

SOC— State-of-charge

SOF— State-of-function

SOH— State-of-health

SPI— Serial peripheral interface

SPS— Samples per second

TCR— Temperature coefficient of resistance

TVS— Transient voltage suppression (diodes)

VISA— Virtual Instrument Software Architecture

9 About the Author

SANDEEP TALLADA is a systems engineer at Texas Instruments. As a member of the Automotive Systems Engineering team, Sandeep focuses on HEV/EV, powertrain end-equipments and creating subsystem reference designs. He brings to this role experience in sensor systems technology. Sandeep earned his master of science in sensor systems technology from the University of Applied Sciences Karlsruhe, Germany.

Revision History A

NOTE: Page numbers for previous revisions may differ from page numbers in the current version.

Changes from Original (Oct 2017) to A Revision	Page
• Updated instance of "MSP430F2259" to "MSP430F5529"	2
• Updated instance of "MSP430F2259" to "MSP430F5529"	29

IMPORTANT NOTICE FOR TI DESIGN INFORMATION AND RESOURCES

Texas Instruments Incorporated ('TI") technical, application or other design advice, services or information, including, but not limited to, reference designs and materials relating to evaluation modules, (collectively, "TI Resources") are intended to assist designers who are developing applications that incorporate TI products; by downloading, accessing or using any particular TI Resource in any way, you (individually or, if you are acting on behalf of a company, your company) agree to use it solely for this purpose and subject to the terms of this Notice.

TI's provision of TI Resources does not expand or otherwise alter TI's applicable published warranties or warranty disclaimers for TI products, and no additional obligations or liabilities arise from TI providing such TI Resources. TI reserves the right to make corrections, enhancements, improvements and other changes to its TI Resources.

You understand and agree that you remain responsible for using your independent analysis, evaluation and judgment in designing your applications and that you have full and exclusive responsibility to assure the safety of your applications and compliance of your applications (and of all TI products used in or for your applications) with all applicable regulations, laws and other applicable requirements. You represent that, with respect to your applications, you have all the necessary expertise to create and implement safeguards that (1) anticipate dangerous consequences of failures, (2) monitor failures and their consequences, and (3) lessen the likelihood of failures that might cause harm and take appropriate actions. You agree that prior to using or distributing any applications that include TI products, you will thoroughly test such applications and the functionality of such TI products as used in such applications. TI has not conducted any testing other than that specifically described in the published documentation for a particular TI Resource.

You are authorized to use, copy and modify any individual TI Resource only in connection with the development of applications that include the TI product(s) identified in such TI Resource. NO OTHER LICENSE, EXPRESS OR IMPLIED, BY ESTOPPEL OR OTHERWISE TO ANY OTHER TI INTELLECTUAL PROPERTY RIGHT, AND NO LICENSE TO ANY TECHNOLOGY OR INTELLECTUAL PROPERTY RIGHT OF TI OR ANY THIRD PARTY IS GRANTED HEREIN, including but not limited to any patent right, copyright, mask work right, or other intellectual property right relating to any combination, machine, or process in which TI products or services are used. Information regarding or referencing third-party products or services does not constitute a license to use such products or services, or a warranty or endorsement thereof. Use of TI Resources may require a license from a third party under the patents or other intellectual property of the third party, or a license from TI under the patents or other intellectual property of TI.

TI RESOURCES ARE PROVIDED "AS IS" AND WITH ALL FAULTS. TI DISCLAIMS ALL OTHER WARRANTIES OR REPRESENTATIONS, EXPRESS OR IMPLIED, REGARDING TI RESOURCES OR USE THEREOF, INCLUDING BUT NOT LIMITED TO ACCURACY OR COMPLETENESS, TITLE, ANY EPIDEMIC FAILURE WARRANTY AND ANY IMPLIED WARRANTIES OF MERCHANTABILITY, FITNESS FOR A PARTICULAR PURPOSE, AND NON-INFRINGEMENT OF ANY THIRD PARTY INTELLECTUAL PROPERTY RIGHTS.

TI SHALL NOT BE LIABLE FOR AND SHALL NOT DEFEND OR INDEMNIFY YOU AGAINST ANY CLAIM, INCLUDING BUT NOT LIMITED TO ANY INFRINGEMENT CLAIM THAT RELATES TO OR IS BASED ON ANY COMBINATION OF PRODUCTS EVEN IF DESCRIBED IN TI RESOURCES OR OTHERWISE. IN NO EVENT SHALL TI BE LIABLE FOR ANY ACTUAL, DIRECT, SPECIAL, COLLATERAL, INDIRECT, PUNITIVE, INCIDENTAL, CONSEQUENTIAL OR EXEMPLARY DAMAGES IN CONNECTION WITH OR ARISING OUT OF TI RESOURCES OR USE THEREOF, AND REGARDLESS OF WHETHER TI HAS BEEN ADVISED OF THE POSSIBILITY OF SUCH DAMAGES.

You agree to fully indemnify TI and its representatives against any damages, costs, losses, and/or liabilities arising out of your non-compliance with the terms and provisions of this Notice.

This Notice applies to TI Resources. Additional terms apply to the use and purchase of certain types of materials, TI products and services. These include; without limitation, TI's standard terms for semiconductor products http://www.ti.com/sc/docs/stdterms.htm), evaluation modules, and samples (http://www.ti.com/sc/docs/sampterms.htm).

Mailing Address: Texas Instruments, Post Office Box 655303, Dallas, Texas 75265